Studies on Development of New Surgical Techniques for Dog with Spinal Instability Associated with Degenerative Intervertebral Disc Changes
（椎間板変性が関連する犬の脊椎不安定症に対する新しい手術法の開発に関する研究）

2021

The United Graduate School of Veterinary Sciences
, Gifu University
(Gifu University)

FUJIOKA, Toru

Studies on Development of New Surgical Techniques for Dog with Spinal Instability Associated with Degenerative Intervertebral Disc Changes
（椎間板変性が関連する犬の脊椎不安定症に対する新しい手術法の開発に関する研究）

FUJIOKA, Toru

Contents

Chapter 3

Accuracy and efficacy of a patient-specific drill guide template system for lumbosacral junction fixation in medium and small dogs: cadaveric study and clinical cases

Chapter 4

List of Abbreviations

ACDF : anterior cervical decompression and fusion

AF : annulus fibrosus

ASD : adjacent segment disease

CAD : computer-aided design

CAM : computer-aided manufacturing

CAS : computer-assisted surgery

CSLP : cervical spine locking plate

CSM : cervical spondylomyelopathy

CT : computed tomography

DA-CSM : Disk-associated cervical spondylomyelopathy

DH : disk height

DHI : disk height index

DICOM : Digital Imaging and Communication in Medicine

DLSS : degenerative lumbosacral stenosis

DLW : dorsal lamina width

DLWI : dorsal lamina width index

FW : foramen width

FWI : foramen width index

IVD : intervertebral disc

LCP : locking compression plates

MFS : modified Frankel score

MPR : multi-planar reconstruction

MRI : magnetic resonance imaging

NP：nucleus pulposus

PMMA：polymethylmethacrylate

PSRF：pedicle screw-rod fixation

SOP：string of pearls plates

STL：Standard Triangulated Language

TZ：transition zone

3D：three-dimensional

3D PDG：3-dimensional patient-specific drill guides

General Introduction

Biomechanical function of the intervertebral disc and spinal segment

The intervertebral discs (IVD), ligaments, intervertebral joints, and vertebrae constitute the spine in dogs and are subjected to various movements and loads during motion, such as axial compression, shear tension, tensile force, bending, and torsion（97, 123）. In dogs, the spine is subjected to pressure exerted horizontally and longitudinally by contract of the trunk muscles and tension of the ligaments because it is positioned horizontally to the ground（97, 126）. The biomechanical functions of the IVD is to disperse and transmit intervertebral compressive force to vertebral bodies in order to provide stability and mobility to the spine（3, 80）. The nucleus pulposus (NP), annulus fibrosus (AF), transition zone (TZ), and vertebral end plate are functional units that supports resistance to spinal movements and loads, and each of them has a different and specialized function（86, 93）. The NP is a highly hydrated structure that influences swelling pressure inside the IVD. The NP and inner TZ absorb the majority of the compressive load when pressure is exerted on the trunk axis. The surrounding AF protects the NP from the applied load and shear tension, and maintains the circumference of the IVD（3）.

Pathology of spinal instability associated with disc degeneration in dogs

Spinal instability in dogs develops as a result of a wide variety of pathological conditions, including degenerative change of the IVD, trauma, congenital malformation, and other pathological processes such as tumors and infection（44）. Among these conditions, degeneration and protrusion/extrusion of the IVD are the most common causative factor of spinal instability and spinal cord compression in dogs（15, 22, 69）. Genetic predisposition, chronic biomechanical overload and trauma, and improper metabolism are factors involved in degeneration of the IVD（2, 17）. The normal NP tissue is composed of notochordal cells and chondrocyte-like cells（49）. As the NP degenerates, notochordal cells are eliminated and water content decreases, and notochordal cells are replaced by fibrochondrocyte-like cells（14, 77）. Once the NP decreases in size due to dehydration in this manner, the NP no longer has its normal capacity of absorbing compressive load. The compressive load-bearing function, which is normally the role of the NP, is taken over by the AF（1, 67）. Then, the AF increases in size, decreases in strength, and undergoes structural deterioration such that the AF loses resistance to tensile forces（2）. Structural damage to the AF can cause the formation of annular defects and cracks, through which degenerated NP can be pushed out（2, 43）. Furthermore, structural damage and subsequent degeneration of the NP and AF result in uneven load to the vertebral end plate, thereby making the vertebral end plate more susceptible to injury（40）. As such, degeneration of the IVD impacts not only the IVD function but also functions of various other components of the spine, such as ligaments, intervertebral joints, and vertebra（2）. Malfunction of IVD increases mechanical load on intervertebral joints due to spinal movement（10, 53）, and changes in the loading pattern on intervertebral joints also affects the adjacent vertebral bodies to induce sclerosis and spondylosis of the vertebral bodies（57）. In the final stage of IVD degeneration, reduction of laxity and loss of flexibility of the spine are observed, and narrowing of the IVD spaces and osteophyte formation, which are observed in osteoarthritis of the spine, result from restabilization of the spine（36, 99）. Studies in humans suggested that early IVD degeneration is associated with instability of the affected spine, whereas advanced disc degeneration is associated with an increase in stiffness of the spine（25, 26, 59）. The deficits of the biomechanical quality and integrity of the spine due to IVD degeneration cause structural damage to functional vertebral segments, and eventually induce various degrees of spinal cord compression（69）. In dogs with IVD degeneration, Hansen type I disc herniation is frequently observed in the cervical and thoracolumbar regions（43）, whereas Hansen type II disc herniation have been widely known to be a cause of cervical spondylomyelopathy (CSM) and degenerative lumbosacral stenosis (DLSS)（69）.

In disc associated cervical spondylomyelopathy (DA-CSM), osteogenic components around the IVD, ligamentum flavum and articular processes, and soft tissues, such as the articular capsule of the facet joint, compress the spinal cord at a single or multiple site, causing damage to important organs of the nervous and vascular systems（111）. Although the exact pathophysiology has yet to be determined, spinal instability due to DA-CSM has been considered to induce hypertrophy of soft tissues and bony structures and degeneration of IVD, leading to spinal cord compression and chronic progressive myelopathy（44）.

DLSS is the most frequent cause of lumbosacral disease in dogs（61, 117）. Repeated physical overload on the lumbosacral IVD or genetic predisposition may cause IVD degeneration and subsequent instability of the lumbosacral spine（100）. Lumbosacral instability eventually causes degenerative changes in adjacent bony and soft tissue structures, such as the articular capsule of the facet joint, dorsal ligamentum flavum, and L7 and S1 vertebral bodies and endplates. These degenerative changes may cause vertebral canal stenosis and cauda equina compression（30, 61, 121）.

Surgical treatment of spinal instability

Surgical treatment for spinal instability aims at decompression of the spinal cord and/or cauda equina and subsequent spinal stabilization. Surgical stabilization of the spine in dogs has been widely supported for improving a wide variety of clinical signs due to spinal instability caused by degenerative diseases such as DA-CSM and DLSS（44, 79）, fracture and luxation, congenital anomalies（5）, infectious diseases, such as discospondylitis（6）, and neoplasms（31）. Reported spinal stabilization techniques involving implant placement in the pedicles and/or vertebral bodies include the use of pins or screws with polymethylmethacrylate (PMMA)（12, 35, 63, 65, 107）, vertebral body plate（11, 114）, string of pearls plates (SOP)（34）, clamp rod internal fixator（115）, and external skeletal spinal fixation（119, 120）.

Stabilization of the canine caudal cervical spine

Stabilization of the canine caudal cervical spine has been generally performed for the treatment of instability caused by trauma and DA-CSM（11, 13, 35, 114）. In particular, surgical stabilization of DA-CSM in dogs has been considered an effective treatment option and frequently referred to as a model of human cervical spinal disorders（11, 101, 102, 112）. Among the procedures of surgical stabilization of the canine cervical spine, PMMA fixation with bi-cortical placement of pins or screws in the vertebral bodies adjacent to the affected intervertebral joint has been regarded as an established surgical technique （16）. While bi-cortical implant placement is biomechanically advantageous for stiffness, implementation of this procedure may cause damage to the spinal cord by perforating the vertebral canal , vertebral artery and nerve roots during surgery in the canine cervical spine, and to the abdominal aorta during surgery in the canine thoracolumbar spine（44）. According to a study that confirmed the mobility of the cadaveric canine cervical spine in which implants were placed in stabilized intervertebral motion units, the frequencies of protrusion of pins into the intervertebral foramen (vertebral canal or transverse foramen) were ≥57% when positive profile threaded pins were inserted laterally, 25% using smooth pins, and 41% in all cases（58）. In another study which compared the biomechanics of bi-cortical pins and mono-cortical screws placed free-hand in the canine cervical spine, violation of the vertebral canal was milder with mono-cortical screw fixation, whereas vertebral canal violation was observed in 100% with bi-cortical pins（45）. Therefore, conventional bi-cortical implant placement is no longer recommended due to this unacceptable risk of vertebral canal violation, and the use of mono-cortical implants should be considered in surgery for the canine cervical spine（44）. Under such circumstances, implants with a mono-cortical locking mechanism, which are expected to reduce the risk of implant loosening and damage of important organs, have been introduced, and lower profile implants, such as SOP, may replace fixation techniques using PMMA. When locking plates and locking screws are used in the canine cervical spine, they are placed mono-cortically and the locking screws are slightly angulated medially, with their trajectories converging without perforating the transverse foramen or vertebral canal, considerably reducing the risk of damaging the vertebral artery and/or nerve roots（112）. In addition, reports in which mono-cortical screws with locking plates or PMMA were applied in dogs support the use of these methods as clinically and biomechanically superior techniques compared to those with bi-cortical pins or screws with PMMA（4, 11, 45, 90, 102, 112, 114）.

Spinal cord compression may be reduced by cervical spine distraction-stabilization techniques which restore the width of the IVD space, flatten excess soft tissues such as the dorsal ligamentum flavum and articular capsule, and widen the narrowed intervertebral foramen（112）. Seim and Withrow who classified CSM in 1982 as a chronic degenerative IVD disease emphasized that linear distraction of the cervical spine is very important to improve the narrowed IVD space and intervertebral foramen, and compression of the spinal cord by excess soft tissues（92）. Therefore, when cervical spine instability due to DA-CSM is suspected, a treatment option is intervertebral distraction and stabilization.

Short-term stability can be achieved by implant fixation, but the eventual goal of intervertebral stabilization for long term stability is bony fusion across the affected intervertebral articulation（44）. Distraction-stabilization techniques have been performed by the combined use of screws, pins, and plates with autologous bone fragments（11, 24, 112）, PMMA cement plugs（24）, and other metallic intervertebral implants such as washers（24）, customized devices（52）, and spacers（85, 101, 102）. Additionally, spinal fusion is currently considered to be the gold standard of surgical treatment for CSM in dogs（7, 8）. As lifetime stability cannot be provided using the implants alone, bony bridging between endplates of vertebral bodies is the goal of surgical treatment（84）. However, in these distraction-stabilization techniques, early implant failure associated with loss of vertebral distraction before bony fusion is the most frequent cause of failure（16, 32, 39, 58, 63, 65, 81）.

In the 1950s, Robinson and Smith introduced anterior cervical decompression and fusion (ACDF) for human with CSM, and early implant failure has since been reported with dissemination of the technique. To improve destructive complications occasionally observed during fixation of a single or multiple cervical joints, many intervertebral spacers, screws, and plates have been developed in human medicine（54, 83, 89, 95, 96, 112, 125）. ACDF using cylindrical titanium spacers is an established surgical technique for human with CSM（73, 75）. Titanium spacers are less frequently associated with the risk of intervertebral collapse or subsidence of implants into the endplates, unlike autologous bone grafts or hydroxyl apatite, and are expected to consistently result in more ideal postoperative spinal alignment（48）. ACDF using titanium spacers was reported in Japan in 1997 and has since been widely accepted（48）. However, long-term follow-up studies of ACDF using titanium spacers reported postoperative subsidence of the spacers, adjacent disc disease (ASD), and kyphotic deformity（46, 104）. Thus, many techniques and implants have been developed for stabilization-fusion techniques of the cervical spine in human medicine, but few implants for the canine cervical spine have been developed and most of them were reported based on case reports or only a small number of biomechanical studies. (11, 84, 101, 102, 112)

In the canine cervical spine, the distraction-stabilization technique using the intervertebral spacer and locking plate is becoming a mainstay, but previous reports of its use are limited, and the effectiveness of the distraction-stabilization technique is evaluated only by clinical findings and radiography without morphometric analysis of the degree of distraction. Additionally, early implant failure and subsidence with loss of vertebral distraction before bony fusion have been the most common cause of failure in the distraction-stabilization technique.

Stabilization of the canine thoracolumbar spine and lumbosacral spine

The thoracolumbar spine and lumbosacral spine in dogs have been stabilized by inserting pins or screws into the pedicles or vertebral bodies, followed by fixation with PMMA or placement of vertebral body plates (122). The combination of bi-cortical pins or screws and PMMA has been established as a technique for the treatment of instability of the cervical and thoracolumbar and lumbosacral spine in middle-sized and large dogs, but standard orthopedic implants and common human implants of neurosurgery have also been applied in spinal fixation in dogs (74). Locking compression plates (LCP) (103), SOP (34, 76), and pedicle screw-rod fixation (PSRF) (100, 108, 127) are replacing spinal fixation using pins or screws and PMMA as a technique for stabilization of the thoracolumbar and lumbosacral spine in dogs. However, when using LCP or SOP for fixation of the thoracolumbar or lumbosacral spine in dogs, implant placement with insufficient stiffness has the risk of implant failure and complications（11, 112）. As PSRF is an implant system developed for human use and not for veterinary neurosurgery, it cannot be applied to thoracolumbar or lumbosacral spine fixation in dogs of all sizes. On the other hand, pins or screws and PMMA can be applied in dogs of all sizes and provide rigid fixation（12, 51）. Therefore, the use of pins or screws in combination PMMA has been the standard technique for the stabilization of the thoracolumbar and lumbosacral spine in dogs. Ideal trajectories of screw/pin insertion and landmarks were previously reported for the placement of bi-cortical implants to the canine cervical, thoracolumbar and lumbosacral spine（116）. However, there is the possibility of iatrogenic damage to vital structures, such as the vertebral canal, nerve roots, and blood vessels, during free-hand insertion of pins or screws into the thoracolumbar or lumbosacral spine（4, 112, 114）.

The objective of this study was to develop safe and effective surgical procedures for canine caudal cervical, thoracolumbar and lumbosacral spinal instability caused by degenerative IVD disease in dogs.

In Chapter 1 the purpose of the study was to evaluate the efficacy and safety of distraction and fusion techniques combining a cylindrical spacer and locking plates (mono-cortical) in 6 dogs with DA-CSM. To evaluate the degree of spinal distraction before and after surgery, I performed morphometric analysis of CT images of dogs that underwent surgery to assess the effects of distraction and followed up clinical findings and radiography to assess the safety. I also investigated the incidence of complications including implant failure, subsidence of the intervertebral spacer, and adjacent IVD lesions in addition to intervertebral bony fusion.

In Chapters 2 and 3, I evaluated the accuracy and safety of a new surgical technique using a patient -specific drill guide template system as intraoperative support for instability of the thoracolumbar and lumbosacral spine in dogs. The objective of these studies was to develop the intraoperative support device that can be used to safely perform spinal stabilization using pins or screws and PMMA. The accuracy and safety of the new drill guide template were evaluated in cadaveric spines, and in the thoracolumbar and lumbosacral spine in clinical cases.

Chapter 1

Morphometric evaluation of the effect of distraction and fusion surgery in dogs with disc-associated cervical spondylomyelopathy.

Introduction

DA-CSM is a disease in which cervical spine instability occurs following IVD degeneration. Consequently, the spinal cord is compressed by supporting tissues such as the protruded/extruded IVD, hypertrophic ligamentum flavum and articular process joint capsules（50, 91, 113）. Surgical treatment is aimed at decompressing the spinal cord and stabilizing the cervical vertebrae. Ventral slot has been performed for decompression of the cervical spinal cord, and various implants for stabilization of the cervical spine have been reported（32, 35, 50, 58, 65, 81, 87）. Regarding the stabilization of the cervical spine, many surgical techniques have been reported, including interbody implants such as PMMA cement plugs, allogenic cortical bone grafts, customized devices, or other intervertebral spacers combined with pins or screws and PMMA or plates（11, 24, 52, 101, 102, 112）.

In recent years, distraction-stabilization techniques using an intervertebral spacer in combination with a locking plate have been reported in veterinary medicine（11, 84, 101, 102, 112）. The advantage of the intervertebral spacer is its ability to distract the disc space and provide load sharing between adjacent vertebral endplates（11, 52, 84, 101, 102, 112）. However, to date, the effect of intervertebral spacer has not been verified in terms of the degree of spinal decompression and intervertebral distraction in dogs.

The purpose of this preliminary clinical study was to evaluate the effects of distraction and fusion technique using an intervertebral spacer and locking plates on clinical and imaging outcomes in 6 dogs with DA-CSM. Spinal fusion was examined with radiography and CT. In addition, the effect of insertion of the intervertebral spacer was evaluated by imaging follow-up and morphometric analyses.

Materials and Methods

Case Enrollment

This study was conducted as a retrospective multi-institutional clinical study performed on client-owned dogs with DA-CSM. Imaging studies and surgical procedures were performed at either a private animal hospital or a university teaching animal hospital with the informed consent of the dog owners. All procedures were performed in accordance with the guidelines regulating animal use and ethics at Gifu University and approved by the Animal care center of Gifu University and Use Committee (approval No. 15062).

Cases

Dogs diagnosed as DA-CSM in the teaching hospital of Gifu University and Ivy Animal Clinic between March 2015 and October 2017 were included in this study. A diagnosis of DA-CSM was based on neurological examination, radiography, myelography, CT (Alexion Advance; Canon Medical System Corporation, Tochigi, Japan or ECLOS-8S; Hitachi Healthcare, Tokyo, Japan), and/or MRI (0.4-Tesla APERTO Eterna; Hitachi Healthcare, Tokyo, Japan or 0.3-Tesla AIRIS Vento LT; Hitachi Healthcare, Tokyo, Japan). All dogs were treated with a combination of an intervertebral spacer and ventrally placed locking plates. Signalment, clinical signs, diagnostic procedures, surgical findings, and clinical outcome of each case were recorded.

Neurological assessment

Neurologic grading was defined as previously reported (87). Neurologic grading was defined as 0 (normal neurologic examination), 1 (cervical pain during manipulation), 2 (mild pelvic limb ataxia with no proprioceptive deficits), 3 (mild ambulatory tetraparesis), 4 (severe ambulatory tetraparesis), and 5 (nonambulatory tetraparesis). Dogs were assessed at pre-surgery, perioperative period (0-3ms), short-follow-up period (3-6ms), mid follow-up period (6-12ms), long follow-up period (>12ms) (20).

Implants

The cylindrical intervertebral spacer (m-cage; Ammtec Inc., Tokyo, Japan) was used as a fusion spacer (Fig. 1-1), and locking plates (Matrix mandible plating system; DePuy Synthes Johnson & Johnson, Tokyo, Japan) and screws (Matrix mandible plating system; DePuy Synthes Johnson & Johnson, Tokyo, Japan) were used for vertebral body fixation. The spacer was a titanium cylindrical spacer made of Ti6Al4V with 5mm in an inner diameter and 7.5mm in an outer diameter, 12mm length. The spacer had a central slot 3.0mm wide for filling up cancellous bone and had small circular holes for bone invasion from vertebral body endplates.

Preoperative Imaging

Preoperative diagnostic imaging for all dogs was performed by radiography, CT, and MRI of the cervical spine. In some cases, myelography and dynamic MRI was performed. All dogs underwent immediate postoperative CT and MRI to evaluate the implant position and the degree of decompression of the spinal cord.

Simulation of implant placement

CT images with a slice thickness of 0.5-1.0 mm were used to obtain preoperative images of the cervical spine. Images were imported as the 'Digital Imaging and Communication in Medicine' (DICOM) format to 3D/multiplanar imaging software (OsiriX; Pixmeo SARL, Bernex, Switzerland) and the DICOM data were converted to the 'Standard Triangulated Language' (STL) format to fabricate a patient-specific cervical vertebral model using a 3D printing system (Form 2; Formlabs, Somerville, MA, USA). Using the model, locking plates were contoured to the ventral surface of the affected cervical vertebrae and screw trajectory was assessed to avoid injuries to the vertebral canal, transverse foramen, intervertebral foramen, and IVD (Fig. 1-2). The simulation of implant placement was performed in all cases.

Surgical Procedure

All dogs were positioned in dorsal recumbency on a vacuum positioner with the neck slightly extended. The surgical area was prepared and draped, including the cranial cervical spine and bilateral proximal humerus. In all cases, autologous cancellous bone was harvested from the proximal humerus for bone grafting. The ventral approach for cervical spine was performed as previously reported（122）. The longus colli muscles were retracted by Gelpi retractor to expose the affected IVD space and the ventral aspect of the vertebral bodies.

After a portion of the ventral annulus of the affected IVD was removed by tumor forceps (Masters-ring tumor forceps; Mizuho Inc., Tokyo, Japan) to expose the cranial and caudal endplate surfaces, a vertebral spreader (CLOWARD ventral spreader; Muranaka Inc., Osaka, Japan) was inserted into the affected IVD space and the distraction of vertebrae was performed for discectomy. A portion of the dorsal annulus fibrosus and the dorsal longitudinal ligament were removed to decompress the spinal cord and the dura mater of the spinal cord was exposed. Prior to spacer insertion, the spacer slot was packed with autologous cancellous bone harvested from the proximal humerus. After removing the spreader, the spacer was held by a custom applicator and screwed in while biting into the cranial and caudal endplates of the affected IVD space. Burring of the end plate was not performed. The depth of the spacer insertion was confirmed by fluoroscopy (BV Endura; PHILIPS, Tokyo, Japan) so that the spacer seated just below the dorsal cortex of the vertebral bodies. Dogs with multiple affected sites received a spacer at each site. The vertebral body fixation was performed by double ventral plating by using the pre-contoured locking plates and screws in a mono-cortical fashion. Autologous bone graft was placed around the plates and over the ventral aspect of the spacer (Fig. 1-3).

Post-operative care

Postoperatively, neurological status and urinary bladder function were monitored and dogs received analgesia management, and frequent turning if non-ambulatory. Immediately following surgery, icing of the surgical site and physiotherapy were initiated. Physiotherapy included standing proprioceptive feedback and passive range of motion exercises. Postoperative analgesia during hospitalization was provided by constant rate infusion of fentanyl (5 μg/kg/h) and ketamine (0.4 mg/kg/h). In addition, dogs were given carprofen (4.4 mg/kg PO) or robenacoxib (2 mg/kg SC) once daily. A neck brace was not used. All cases were discharged within a week post-surgery. Postoperative recommendations included leash or harness restraint walks for 2 to 4 weeks post-surgery if there was no ataxia or paresis.

Clinical follow-up

Peri-operative (0-3months), short-term (3-6months), mid-term (6-12 months), and long-term (>12 months) post-operative follow-up evaluations (20) consisted of physical and neurological examinations. In 2 cases (Case No.2 and 6), a telephone interview was performed in order to assess mid-term and/or long-term outcomes.

Imaging follow-up

Post-operative radiographs were performed at peri-operative follow-up period (0-3months), short follow-up period (3-6months), mid follow-up period (6-12 months), and long follow-up period (>12 months). Postoperative CT were performed at peri-operative follow-up period, short follow-up period, mid follow-up period, and long follow-up period. CT images were assessed for the presence of bridging bone around the intervertebral spacer and/or the vertebral bodies, implant failure (i.e., screw loosening, plate dislocation, and screw or plate breakage), and invasion of the spacer into the vertebral canal. Subsidence of the intervertebral spacer was assessed by measuring the linear distance between the center of the cranial endplate of the vertebral body and the center of the caudal endplate of the vertebral body including the interposed disc space（84）. Evaluation of bony fusion was performed as previously reported（11, 84, 101, 102, 112）. Mid and long-term follow-up MRI for 2 cases (Case No. 3 and 5) were assessed using the modified Pfirmann score for grading the degenerative changes in the adjacent segment of the affected IVD（9）.

Morphometric Analyses

Morphometric analyses were performed by using CT images at pre-surgery and immediately post-surgery for 8 affected IVD spaces in 6 dogs. Pre- and post-operative CT images were exported in the DICOM format to imaging software. Disc height (DH) and foramen width (FW) were measured and disc height index (DHI) (Fig. 1-4A and 1-4B) and foramen width index (FWI) (Fig. 1-4C and 1-4D) were calculated according to the previously reported methods （82, 109）. Dorsal lamina width (DLW) and dorsal lamina width index (DLWI) were measured in order to evaluate distraction of the dorsal lamina space by the intervertebral spacer. DLWI was calculated by dividing the width between the cranial and caudal dorsal lamina by the average length of the cranial and caudal vertebral body lengths (Fig. 1-4E and 1-4F).

Statistical Analyses

The differences between the mean values of DHI, FWI, and DLWI between different time points were statistically compared. All statistical analyses were performed with a paired t-test by JMP (SAS Institute Japan, Tokyo, Japan). Statistical significance was set at $p < 0.05$.

Results

Case Population

Clinical information of all cases is summarized in Table 1-1. The median age at the first visit of the 6 dogs was 86.5 months (range, 29-132 months). The median age at surgery was 87 months (range, 30-133 months). The median body weight at surgery was 32.6kg (range, 27.8-40.0 kg). Breeds included Doberman pinscher (3), Bernese mountain dog (2), and Weimaraner (1). Five dogs had chronic progressive clinical signs, and 1 dog (Case No. 2) presented with an acute onset of clinical signs three days prior to presentation. Clinical signs at presentation were mild ambulatory tetraparesis (n=3) and severe ambulatory tetraparesis (n=3).

Preoperative imaging findings

Imaging findings, diagnosis, surgical site are summarized in Table 1-1. Spinal cord compression was caused by IVD protrusion in combination with dorsal ligamentum flavum compression in all dogs. DA-CSM involved a single lesion in 4 dogs and multiple lesions in 2 dogs. In all dogs, degenerative changes of the adjacent IVD were confirmed by MRI. One dog (Case No. 4) had a dorsal arachnoid diverticulum at the affected intervertebral disc level and another dog (Case No. 5) had a partial calcification of the intervertebral disc at C5-6 cranial to the surgical site of C6-7.

Surgery and complications

After the diagnosis of DA-CSM by MRI (Fig. 1-5A), surgical treatment involved removal of the dorsal annulus fibrosis and the dorsal longitudinal ligament of the affected IVD followed by insertion of the intervertebral spacer. The spacer slot was packed with autologous cancellous bone harvested from the proximal humerus. Two pre-contoured locking plates (2.8 mm in thickness) were applied with mono-cortical self-tapping locking screws (3.0 mm in diameter) and autologous bone graft was placed around and ventral to the plates and over the ventral aspect of the spacer (Fig. 1-5B). Intraoperative complications resulting from screw insertion were assessed by intraoperative fluoroscopy. Postoperative CT images and/or MRI (Fig. 1-5C and 1- 5D) were performed to confirm the degree of spinal cord decompression and the implant position. Median surgical time was 369 minutes (range, 260-480 minutes), and median hospitalization time was 4 days (range, 4-7 days). No major complications related to the surgical procedure were recorded.

Clinical follow-up

Clinical follow-up evaluation of all cases is summarized in Table 1-1. The median follow-up time was 18.8 months (range, 12-34 months). One dog (Case No. 2) died of heart failure, suspected of dilated cardiomyopathy, at 12 months post-surgery. The neurologic scores of all dogs were improved by 3 months post-surgery. Results of mid-term follow-up examination were available for 6 dogs. The neurologic scores of these dogs were improved compared to pre-surgery or to peri-operative period. Four dogs had cervical pain during manipulation. The other 2 dogs had mild pelvic ataxia with no proprioceptive defects. Results of long-term follow-up examination and/or questionnaire (telephone interview) were available for 5 dogs. None of the dogs deteriorated from pre-surgery or from the peri-operative follow-up evaluations.

Imaging follow-up and morphometric analyses

Follow-up radiographs were obtained at perioperative period (n=6), short-term follow-up period (n=6), mid follow-up period (n=4) and long follow-up period (n=2). Follow-up CT imaging were obtained at perioperative period (n=6), short follow-up period (n=1), mid follow-up period (n=2) and long follow-up period (n=2). Follow-up MRI were obtained at perioperative period (n=6), short follow-up period (n=1), mid follow-up period (n=1) and long follow-up period (n=2).

DH, FW, and DLW were measured and their indexes, DHI, FWI, and DLWI were calculated using CT images of pre- and post-surgery (Table 1-2). Significant increases of DHI (Pre, 0.22 ± 0.04; Post, 0.32 ± 0.03; P = 0.001), FWI (Right, (Pre, 0.41 ± 0.04; Post, 0.51 ± 0.05; P=0.004; Left, Pre, 0.42 ± 0.06; Post, 0.51 ± 0.09; P=0.003) at the surgery site were found between pre-surgery and immediately post-surgery. Three affected IVD spaces in 2 dogs (Case No. 3 and 4) for which long-term follow up examinations were performed, the DHI at immediately post-surgery and long-term follow-up period were 0.32 ± 0.02 and 0.21 ± 0.03, respectively. The FWI (right side) at immediately post-surgery and long-term follow-up period were 0.53 ± 0.07and 0.38 ± 0.04, respectively. The FWI (left side) were 0.53 ± 0.05 and 0.40 ± 0.03, respectively. DLWI at immediately post-surgery and long-term follow-up period were 0.29 ± 0.03 and 0.19 ± 0.04, respectively.

Bony fusion was evaluated by radiography and CT imaging. Bridging new bone around the cage was confirmed by radiography in all dogs at short-term follow-up period. In 4 dogs for which mid and long-term follow up CT imaging were performed, formation of bone was seen around the ventral aspect of the vertebral bodies and in the intervertebral spacer in 3 dogs (Case No. 3, 4 and 5) (Fig. 1-6).

Subsidence of the intervertebral spacer was observed on radiographs in 7/8 affected IVD spaces in 5/6 dogs at short-term follow-up period. Subsidence of the intervertebral spacer was observed by mid-term follow-up period in all dogs. The median distance of subsidence at short- and mid-term follow-up period was 1.4 mm (range, 0.1-2.3 mm) and 1.4 mm (range, 0.4-2.8 mm), respectively. None of the 6 dogs showed evidence of spacer migration or screw penetration into the vertebral canal, IVD space and transverse foramen on follow-up imaging.

Implant failure included screw loosening noted at 4 months post-surgery in 1 dog (Case No. 5), broken screws noted at 6 months post-surgery in another dog (Case No. 2), one broken plate noted at 12 months post-surgery, and two broken plates at 18 months post-surgery in another dog (Case No. 3) (Fig.1-7). There was no clinical deterioration associated with these findings, therefore revision surgery was not performed.

In 2 dogs (Case No. 3 and 5) for which long-term follow up MRI were performed, the signal intensity of the adjacent IVD were decreased. In 1 dog (Case No. 3), the sagittal T2-weighted MRI image at 24 months post-surgery showed that the signal intensity of the adjacent IVD (C4-5, C7-T1) to the surgical site at C5-C6-C7 was lower than that of pre-surgery (Fig. 1-8), and compression of the spinal cord at the adjacent IVD (C4-C5) found on MRI was thought to account for the deterioration of clinical findings (neurological grade, 1→2). In the other dog (Case No. 5), the signal intensity of the adjacent IVD (C5-6, C7-T1) in the sagittal T2-weighted MRI image at 8 months post-surgery was lower than that of pre-surgery, and compression of the spinal cord in C5-6 was confirmed. Deterioration of clinical findings was not observed at this point, but at 17 months post-surgery, deterioration of clinical signs was confirmed (Fig. 1-9). These 2 dogs were treated medically with administration of carprofen (4.4 mg/kg PO) or robenacoxib (2 mg/kg SC) for 2 weeks. The clinical sings of these cases improved with medical treatment.

Discussion

Surgical treatments of DA-CSM include dorsal or ventral spinal cord decompression and distraction-stabilization techniques with or without the use of cervical artificial discs（11, 28, 50, 87, 112）. In recent years, ventral distraction-stabilization techniques have been the preferred surgical technique in dogs with cervical instability and associated myelopathy because dynamic spinal cord compression and nerve root compression can be treated（11, 35, 84, 101, 102, 112）. I performed morphometric measurements of the cervical spine between pre- and post-surgery CT images in order to evaluate the distraction effect of the spacer. In all dogs, postoperative follow-up of images shown in Figure 1-5 and the results of spinal morphometric analysis shown in Table 1-2 revealed that ventral and dorsal spinal cord compression and nerve root compression by the surrounding soft tissues were reduced by spacer insertion from the ventral side of the IVD space. In 2 dogs for which long-term follow up examinations were performed, spinal morphometry showed that the distraction effects of the spacer in the affected IVD space decreased compared to immediately post-surgery, but the distraction effect was maintained at the same level as pre-operative state.

Early implant failures with loss of distraction such as implant loosening, implant breakage, implant backout and intervertebral spacer subsidence before bony fusion have been the most common complications associated with distraction-stabilization technique（16, 32, 35, 38, 50, 58, 64, 65, 66, 81, 87）. In my study, a decrease of the mid- and long-term distraction effects of the spacer in the affected IVD spaces is accounted for by subsidence of the spacer. Despite spacer subsidence seen in all cases, clinical improvement was achieved in all cases without recurrence, and this may be due to several reasons. First, I directly removed the ventral elements of the compressing structure, and this approach prevented the spinal cord from being compressed again when the IVD space was reduced due to spacer subsidence. Second, cancellous bone graft in and around the spacer promoted early bone fusion and plate fixation further stabilized the operated IVD space. Cancellous bone autograft has been recommended in other clinical studies on DA-CSM and success rates for bony bridging have varied between 70-90% (11, 94, 102, 112) . In the present study, bridging new bone around the spacer was present in all dogs at short-term follow-up period and extended to the ventral side of the vertebral bodies at mid- and long-term follow-up in 3 dogs. The spacers used in this study was made of titanium (Ti6Al4V), which has high osteoblast-affinity. The small circular side holes of the titanium spacers to which bone ingrowth occurs further support lodging the spacer. Therefore, the osteoconductive properties and the configuration of the spacer had led to minimum subsidence of the spacer and successful bone fusion across operated vertebrae.

ASD is an unresolved condition in both human and veterinary medicine, and it remains unclear whether this disease represents a natural progression of degeneration in adjacent vertebral motor units or a biomechanical process caused by stabilization of the spinal segment or effects of spinal implants (screws and/or plates) on the IVD or endplate (50, 102) . ASD can be caused by progressive spontaneous degeneration of the IVD of ventral fixation that alters the biomechanical load of the adjacent disc (47) . In human clinical studies, postoperative imaging indicated increased motion at segments adjacent to cervical fusion sites (47, 62). In veterinary medicine, distraction-stabilization techniques of the canine vertebral body have been reported to possibly change the mechanical environment and cause diseases, such as ASD (23, 28). The risk of clinically significant ASD occurring post-surgery for the treatment of DA-CSM in dogs has been estimated to be approximately 20% (16, 23, 50, 112). ASD was observed in 2 of 6 dogs in the present study. Two dogs with ASD did not show newly degenerative changes on radiography, such as spondylosis deformans at the segments cranial or caudal to the operative site after surgery. It is not clear from our study whether ASD was caused by the effect of this surgical technique or part of the natural progress of degeneration at an adjacent IVD. Although not proposed in this study, as one of the factors of ASD is the increase in movements of adjacent segments with rigid fixation of the affected vertebrae, techniques stabilizing the adjacent vertebrae with controlled movements (e.g., developing mobile implants) are worth investigating as a substitute for fusion surgery in the future.

The distraction and fusion surgery was considered a clinically effective surgical technique in dogs with cervical spine instability. Morphometric analyses revealed that spinal cord compression and nerve root compression were reduced by intervertebral spacer insertion to the affected IVD space. Stabilization and early bony fusion across the affected disc space were considered important in preventing clinical deterioration due to the reduction of the IVD space, dorsal interlaminar space and intervertebral foramina width.

Limitations of this study include a small cohort of animals, lack of a control, and lack of comparison to other stabilization techniques of the canine cervical spine. Imaging during follow-up varied between each dog and time of imaging. Additionally, histopathological analysis was not performed for evaluation of bony fusion.

Tables and Figures

Table 1-1. Summary data for 6 dogs treated with an intervertebral disc spacer and locking plates

	Signalment		Diagnosis and location		Neurological score					Linear distance(mm)				Subsidence(mm)		Outcome		
																Complications		>12ms
Case No.	Breed	Age (ms)	MRI	Surgical site	Pre-surgery	0-3ms	3-6ms	6-12ms	>12ms	Pre-surgery	Post-surgery	0-3ms	3-6ms	0-3ms	3-6ms	Implants	ASD	
1	Weimaraner	91	DA-CSM(C5-6) Spondylosis deformans(C4-5-6-7)	C5-C6	3	1	1	1	1	52.7	54.8	52.8	-	2	-	None	-	Full function
2	Doberman	102	DA-CSM(C5-6-7) Spondylosis deformans(C4-5-6-7)	C5-C6-C7	4	3	2	2*	NE	86.7	98.4	96.8	95.6	0.1	0.2	breakage of screws	-	Dead 12ms(dilated cardiomyopathy)
3	Bernese mountain dog	83	DA-CSM(C5-6-7)	C5-C6-C7	3	2	1	1	2	90.4	100.4	100.3	100.1	1.6	2.8	breakage of screws and plates	C4-5, C7-T1	Acceptable function
4	Bernese mountain dog	78	DA-CSM(C5-6) Spinal arachnoid diverticula(C5-6)	C5-C6	3	1	1	1	1	53.8	57	57	56.6	0	0.4	None	-	Full function
5	Doberman	30	DA-CSM(C6-7) Partial calcification of the intervertebral disc (C5-6)	C6-C7	4	2	1	1	2	54.2	60.8	58.7	58.8	2.1	2	screw loosening	C5-6, C7-T1	Acceptable function
6	Doberman	133	DA-CSM(C5-6) Spondylosis deformans(C6-7)	C5-C6	4	3	2	2	2*	55.2	60.8	58.5	-	2.3	-	None	-	Acceptable function

Neurological grades were as follows: 0, normal neurologic examination; 1, cervical pain during manipulation; 2, mild pelvic limb ataxia with no proprioceptive defects; 3, mild ambulatory tetraparesis; 4, severe ambulatory tetraparesis; 5, non-ambulatory tetraparesis.

Abbreviations: DA-CSM, disc-associated spondylomyelopathy; ms, months; ASD, adjacent segment disease; *, telephone interview; mm, millimeters.

Table 1-2. Comparisons of the mean measured value and index between pre-surgery and post-surgery in 8 affected intervertebral disc spaces for 6 dogs

	DH(mm)	FW(mm)		DLW(mm)	DHI	FWI		DLWI
		R	L			R	L	
Pre-surgery	5.24±0.86	9.51±1.18	9.97±1.71	6.12±1.71	0.22±0.04	0.41±0.04	0.42±0.06	0.26±0.07
Post-surgery	7.73±0.80	11.93±1.58	12.07±2.28	7.48±2.52	0.32±0.03*	0.51±0.05*	0.51±0.09*	0.32±0.11

DH, disc height; DHI, disc height index; FW, foramen width; FWI, foramen width index; DLW, dorsal lamina width; DLWI, dorsal lamina width index; R, right; L, left; mm, millimeters.

*$p < 0.05$

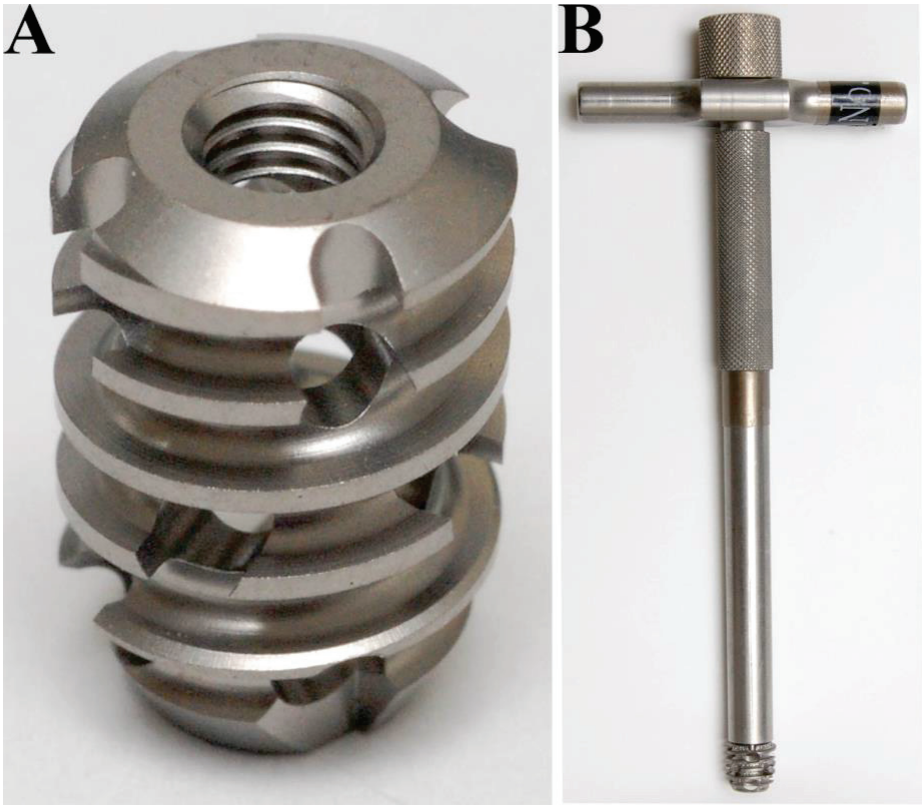

Figure 1-1. The intervertebral spacer is a cylindrical fusion spacer (A) that have a space in middle for bone graft and held by a custom applicator (B)

Figure 1-2. The pre-surgery simulation image of Case No. 5

Pre-contouring of a locking plate was performed with the bone model, which was fabricated before surgery.

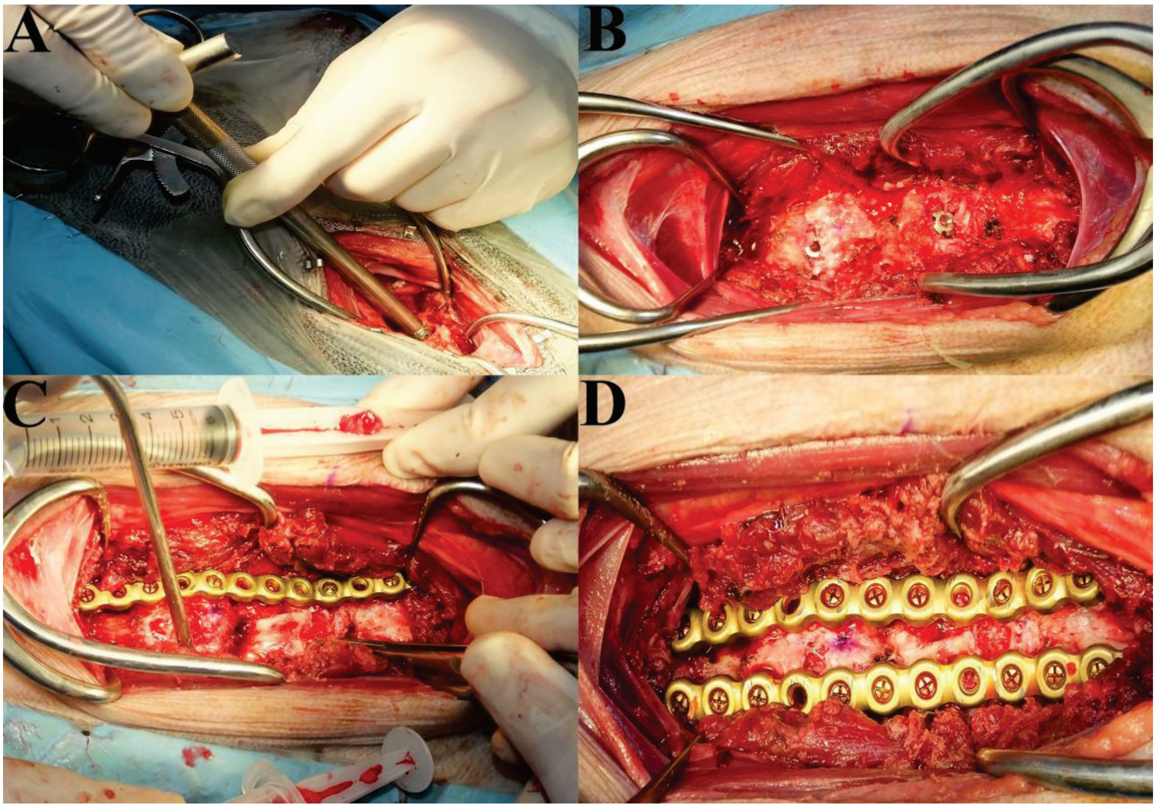

Figure 1-3. Surgical procedure in a representative case (Case No.2)

Insertion of a spacer (A). Ventral view of two inserted spacers at C5-C6-C7 (B). An autologous cancellous bone graft was placed inside the spacer and around the plates (C). Spacer fixation was performed by double locking plates and screws (D).

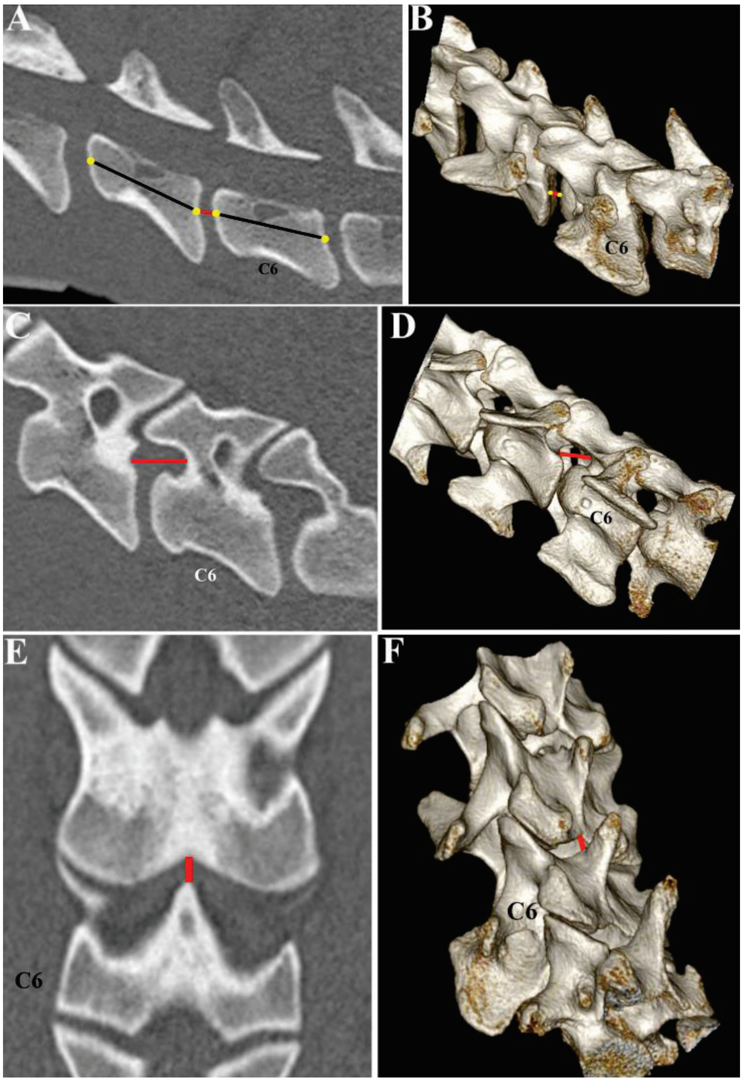

Figure 1-4. Morphometric analysis of C5-C6 from Case No. 2

DHI was calculated by dividing the height of the IVD (red line) by the average length of the cranial and caudal vertebral body lengths (black lines). The center of the cranial and caudal endplates is indicated by solid yellow circles (A, B). FWI was calculated by dividing the intervertebral foramen width (red line) by the average length of the cranial and caudal vertebral body lengths (C, D). DLWI was calculated by dividing the width between the cranial and caudal dorsal lamina (red line) by the average length of the cranial and caudal vertebral body lengths (E, F).

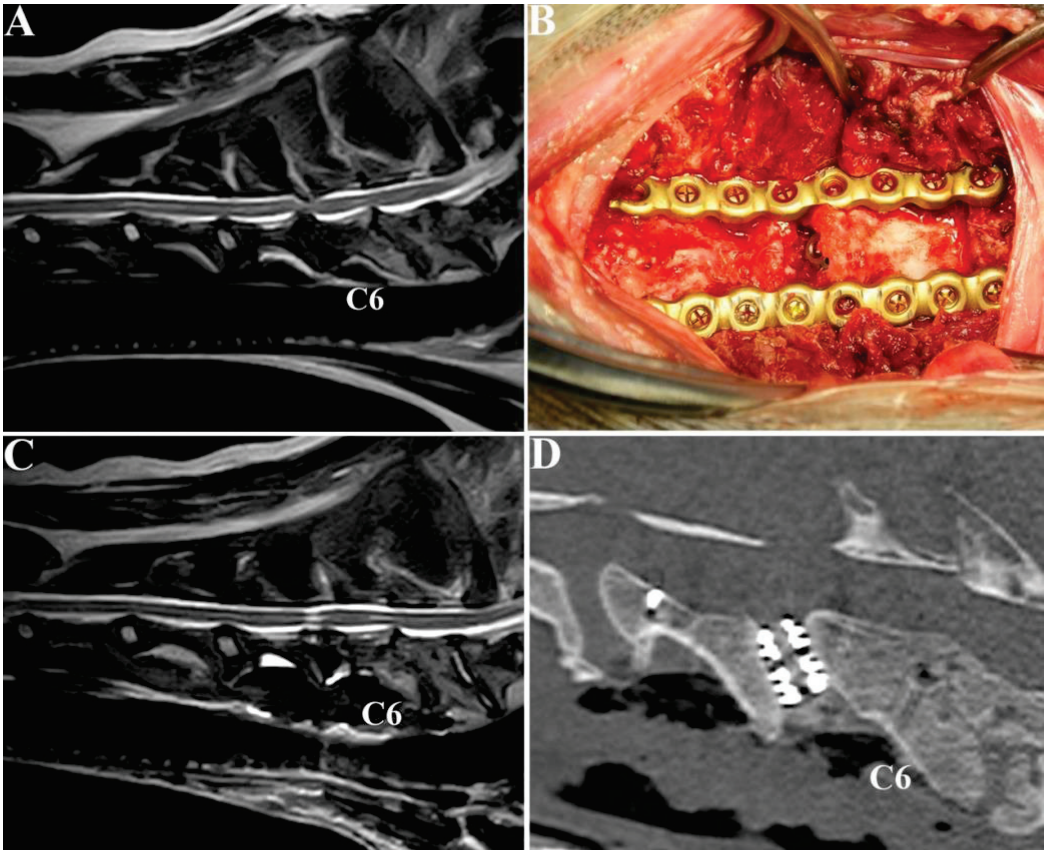

Figure 1-5. Illustration of a representative case (Case No. 6)

Preoperative MRI (A) demonstrated dorsal and ventral compression of the spinal cord at C5-C6. After insertion of an intervertebral spacer was performed, 2 locking plates were placed on the ventral side of C5-6 (B). Postoperative MR (C) and CT (D) images. The inserted spacers distracted the affected IVD space and spinal cord compression at C5-C6 was reduced.

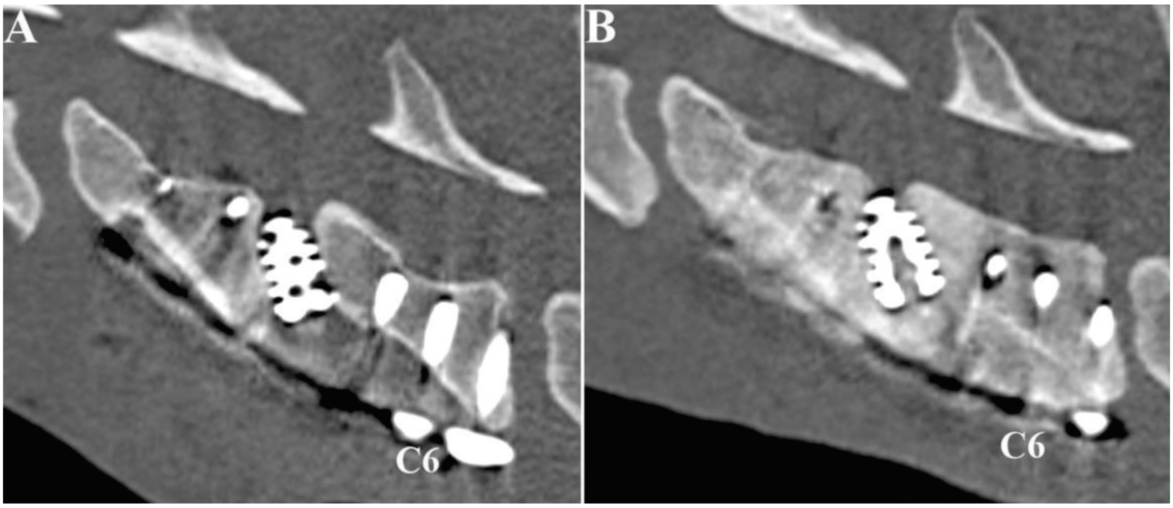

Figure 1-6. One case was confirmed to require bony fusion (Case No. 4)

CT images taken immediately post-surgery (A) and 12 months post-surgery (B). Bone bridging on the ventral side of the vertebral bodies, bone formation in the fusion spacer and subsidence of the spacer were confirmed at 12 months post-surgery.

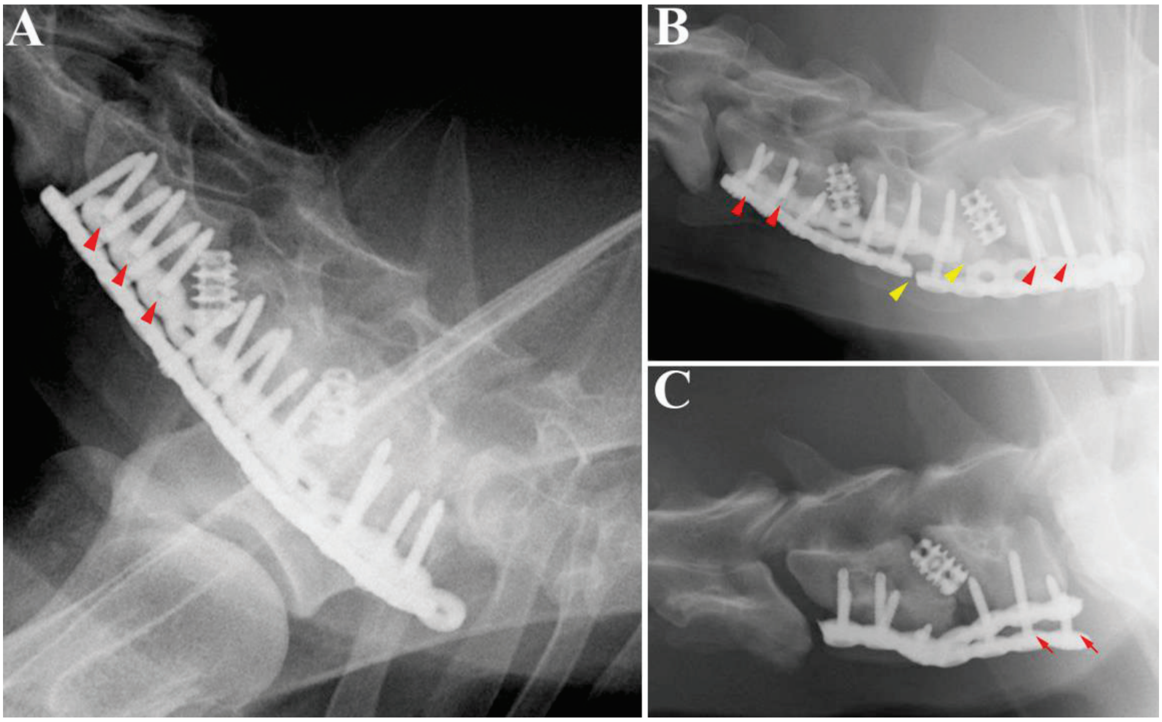

Figure 1-7. Sagittal radiographic images of 3 dogs showing postoperative implants failure

Implant failure included broken screws (red arrowheads) at 6 months post-surgery for Case No. 2 (A), broken screws (red arrows) broken 2 plates (yellow arrowheads) at 18 months post-surgery for Case No. 3 (B), and screw loosening (red arrows) at 3 months post-surgery for Case No. 5 (C).

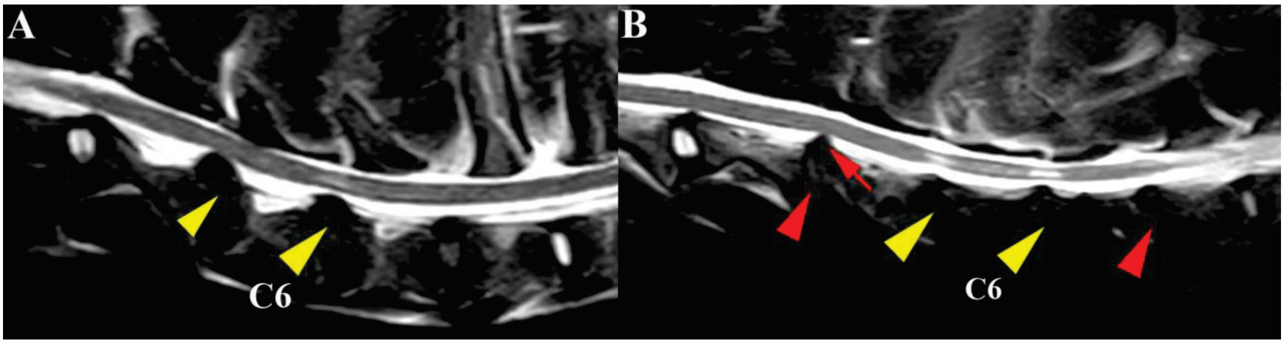

Figure 1-8. Sagittal T2W MRI (Case No. 3)

Preoperative MRI (A), 24 months post-surgery (B). Decreased signal strength in the surgical site of the IVDs and the adjacent intervertebral lesions were confirmed. The yellow arrowheads indicate the surgical sites. The red arrowheads indicate the lower signal intensity in the adjacent IVDs (C4-5, C7-T1). The red arrow indicates the adjacent intervertebral lesions (C4-5).

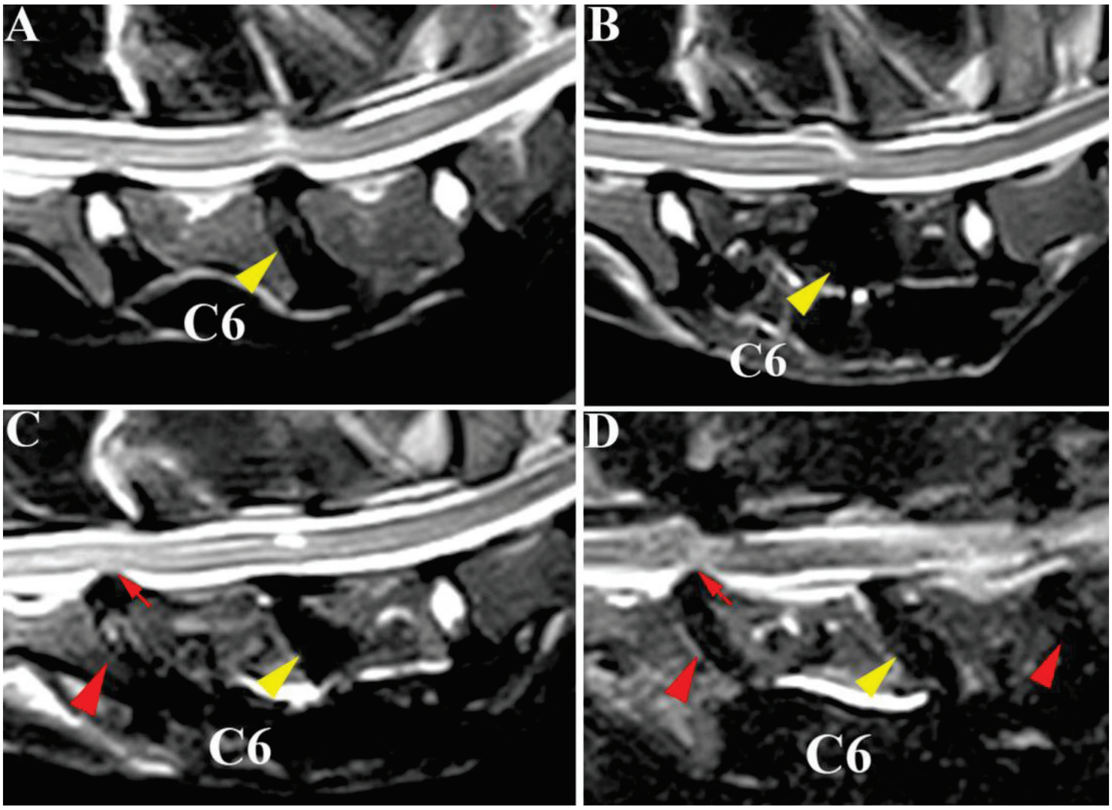

Figure 1-9. Sagittal T2W MRI (Case No. 5).

Preoperative MRI (A), 3 months post-surgery (B), 8 months post-surgery (C), and 17 months post-surgery (D). The yellow arrowheads indicate the surgical sites. The red arrowheads indicate the lower signal intensity in the adjacent IVDs (C5-6, C7-T1). The red arrows indicate the adjacent intervertebral lesions (C5-6).

Chapter 2

A novel patient-specific drill guide template for stabilization of thoracolumbar vertebrae of dogs: cadaveric study and clinical cases.

Introduction

The thoracolumbar spinal instability in dogs is a degenerative and progressive condition in which vertebrae and/or surrounding soft tissues compress the spinal cord dynamically or statically（5, 112）. Clinical signs include pain, ataxia, paresis, paralysis, or a combination of these signs. When clinical signs progress to the point at which quality of life is substantially compromised, the requirement for surgical intervention may need to be considered. Spinal cord decompression followed by vertebral fixation techniques is the treatment of choice for severe cases（5, 102, 112）. Vertebral fixation is achieved by implants, such as pins or screws, placed within the pedicles or vertebral bodies and PMMA, stainless, or titanium plate（41, 45, 74, 102, 103, 108）. In Chapter 1, I demonstrated that distraction and fusion surgery combining an intervertebral spacer and locking plate system is a clinically effective surgical technique in the cervical spine instability. However, when using stainless or titanium plate system for fixation of the thoracolumbar spine in dogs, insertion of screws into the vertebral bodies or pedicles in an ideal trajectory is demanding because the pitch of the screw holes is fixed in each plate and the angulation of the screws is limited. Plates and screws placement with insufficient stiffness has the risk of implant failure and complications（11, 112）. Vertebral fixation by free-hand insertion of pins/screws and PMMA provide rigid fixation and lead to satisfactory outcomes in most clinical cases. Therefore, this procedure has been the standard technique for the stabilization of the thoracolumbar spine in dogs, but carry a potential risk of iatrogenic injury to vital structures including the vasculature, nerve roots, and spinal cord（21, 42, 78）. In humans, free-hand thoracic pedicle screw insertion has been associated with cortical perforation of the pedicles in 44.4-63.8% of cases（19, 110）. Therefore, the accurate placement of implants is of the upmost importance to achieve rigid fixation and also to avoid injury to the surrounding anatomy.

Fluoroscopic guidance and the use of a neuronavigation system have been developed in human medicine, and have significantly improved the accuracy of implant placement（71, 72）. The increased expense of these equipments likely plays a role in their limited adoption in veterinary medicine at the current time, and hence free-hand implant placement is common in spinal fixation surgeries（21, 42）. However, free-hand implantation for spinal fixation may result in iatrogenic injury to the spinal cord, nerve roots, and large vessels, which may lead to serious complications（41, 45, 103）. Additionally anatomical variations in canine vertebrae across different breeds and various malformations in vertebrae make accurate implant placement challenging（21）. Drill guide templates, which have been developed as an inexpensive and accurate method to guide spinal fixation screws in the field of neurosurgery（18, 55, 56, 60）, may be an attractive alternative in veterinary medicine. The increasing number of CT available in veterinary practice and the development of CAD and CAM technology prompted us to evaluate this technology for spinal fixation surgery in dogs（42, 78）.

The objective of the study was to develop the intraoperative support device that can be used to safely perform spinal stabilization using pins or screws and PMMA and to ascertain accuracy and safety of drilling and screw placement using drill guide template in thoracolumbar vertebrae in cadavers and in clinical cases. Furthermore, I reported short and long-term clinical results following thoracolumbar decompression/stabilization in small, client owned dogs.

Materials and Methods

Case Enrollment

This study was conducted as a prospective multi-institutional clinical study performed on client-owned dogs with thoracolumbar spinal instability. Imaging studies and surgical procedures were performed at either a private animal hospital or a teaching animal hospital with the informed consent of the owners. All procedures were performed in accordance with the guidelines regulating animal use and ethics at Gifu University. Sample collection and used for a cadaveric study were approved by Gifu University (approval number: 17211).

Cadaveric Study

Thoracolumbar specimens (T12-L1) were removed from 3 cadavers of adult beagles that were used in other research projects and euthanized for reasons not related to the present study. The median age was 48 months (range: 24-75 months). The median body weight was 11.9 kg (range: 10.7-18 kg). All epaxial muscles were left intact. Spinal specimens were wrapped in saline (0.9% NaCl) solution-soaked paper towels and stored at -20°C until used.

Selection of Screw Trajectories

CT scanners (Alexion Advance, Canon Medical System Corporation, Tochigi, Japan or ECLOS-8S, Hitachi Healthcare, Tokyo, Japan) with a slice thickness of 0.5-1.0 mm were used to obtain preoperative images of the thoracolumbar spine. Images were exported in the DICOM format to 3D/multiplanar imaging software (Ziostation, Ziosoft, Tokyo, Japan) and optimum screw trajectories were selected for each vertebra. Multi-planar reconstruction (MPR) images were prepared from DICOM data, and six trajectories were selected for T12-L1, two trajectories for each vertebra. In the thoracic vertebrae, while confirming the reconstructed image in the cranio-caudal direction, trajectories were planned in order to penetrate the tubercle of the rib for the cranial side or close to the accessory process for the caudal side of the vertebra. I also confirmed on the transverse section that the screws penetrated the vertebral body at an angle of 30-45° against the transverse plane in order to avoid injuries to surrounding important structures (vertebral canals, spinal cord, nerve roots, and blood vessels). In the lumbar vertebrae, trajectories were selected in order for screws to penetrate the vertebral body at an angle of 60-70° against the transverse plane and the base of the transverse process in the cranio-caudal direction (Fig. 2-1).

Design and Fabrication of Custom-Made Drill Guide Templates

Bone data were extracted from DICOM data using image processing software (VG Studio Max, Volume Graphics GmbH, Heidelberg, Germany and Mimics, Materialize, Leuven, Belgium) and transferred to 3D modeling software (Freeform, Data Design, Nagoya, Japan). Bone and drill guide template data were converted to the STL format and fabricated from non-soluble acryl using a 3D printing system (Connex500, Stratasys, Tokyo, Japan) (Fig. 2-2). Drill guide templates comprised 1.5-mm-wide and 12-mm-length cylindrical sleeves extending from the platform that fit the patient-specific 3D shape of the lamina. Small windows were made in the base of the cylindrical structures of the drill guide templates in order to confirm that drilling was performed exactly though the entry point. Patient-specific 3D bone models of the thoracolumbar vertebrae were also made with the same printing system in order to confirm the fit of the templates to the lamina. In each case, I confirmed the fit of the drill guide templates and the corresponding patient–specific 3D bone model and the angle of the drill sleeve to the vertebral body before surgery. The drill guide templates and bone models were sterilized with ethylene oxide gas before surgery.

Surgery

Thoracolumbar vertebral specimens were thawed in warm water before use. The spinous process and lamina arch were exposed by dissecting the epaxial musculature from specimens. Drill guide templates were firmly attached to the lamina by a mosquito forceps and screw holes (bi-cortical) were made with a drill bit (1.5 mm).

Evaluation of the Accuracy and Safety of Drill Guide Templates

Deviations in screw trajectories were assessed using imaging software. Specifically, DICOM data of preoperative and postoperative CT were imported into the software, and three landmarks were registered on the postoperative MPR image. The landmarks used were the spinous process, tubercle of the rib, and intervertebral foramina for the thoracic vertebrae, and the spinous process, transverse process, and intervertebral foramina for the lumbar vertebrae. The fusion of preoperative and postoperative images was performed and the coordinates of the screw holes were identified. Deviations of the coordinates of the entry and exit points on each dimension (x, y, z) were evaluated between the centers of the preoperative and postoperative coordinates and expressed in distance (mm). The deviations were also expressed as percentages where a complete overlap of the planned drill holes and postoperative drill holes corresponded to 0 %. The fusion of images was performed for each vertebra, limited to one vertebra at a time. The X, Y, and Z axes represented the medial-lateral, ventral-dorsal, and cranio-caudal directions, respectively. Screw displacement was graded using postoperative transverse and sagittal CT images as a reference. The safety of drill guide templates was assessed in relation to vertebral canal invasion of the drill hole. Grading of the drill hole trajectory was as follows: Grade 0 (containing), the drill hole trajectory was completely within the wall of the bone structure; Grade 1 (exposure), the drill hole trajectory invaded the wall of the bone structure, while more than 50% of the drill hole diameter remained within the bone; Grade 2 (perforation), the drill hole trajectory invaded the bone structure and more than 50% of the drill hole diameter was outside the bone structure; Grade 3 (penetration), the drill hole trajectory invaded completely outside the bone structure（55）.

Clinical Cases

I performed decompression of the spinal cord and vertebral fixation on 4 dogs (3 pugs and 1 American cocker spaniel). The median age at surgery was 129 months (range: 120-148 months). The median body weight at surgery was 7.5 kg (range: 4.8-10.3 kg). In all clinical cases, I performed a neurological examination, CT imaging, and MRI (0.4-Tesla APERTO Eterna, Hitachi Healthcare, Tokyo, Japan or 0.3-Tesla AIRIS Vento LT, Hitachi Healthcare, Tokyo, Japan). The neurological status of each dog was classified using a modified Frankel score (MFS) (88) . All cases showed chronic progressive paraparesis and ataxia, which were thought to result from spinal instability based on imaging findings of intervertebral disc degeneration, degenerative changes of the vertebrae, or both of these conditions. Clinical information on and the imaging findings of these cases were summarized in Table 2-1.

Surgery

Minihemilaminectomy and/or corpectomy were performed to decompress the spinal cord, depending on the imaging diagnosis. After releasing of the epaxial musculature from the spinous processes, articular processes, and lamina arch of the thoracolumbar spine, the drill guide template was firmly attached to the lamina by a mosquito forceps. A 1.5-mm drill bit was then inserted into the cylinder sleeve and a screw hole was made while visually confirming the entry point from the drill sleeve opening. Consequently, the depth of the screw hole was measured with a depth gauge and cortical bone screws (M 2.0 cortical bone screw, MIZUHO, Tokyo, Japan) with a thread diameter of 2 mm were placed into the vertebral body. The length of the screws was the measurement obtained by the depth gauge plus 10mm. The head of the screw was exposed 10 mm from the lamina surface. One to two screws were placed in each vertebral body (Fig. 2-3). Bone cement (Surgical Simplex P, Stryker, Tokyo, Japan or ENDURANCE, DePuy CMW, Johnson & Johnson company, Tokyo, Japan) was applied in order to cover the screw heads. The locations of the screws were examined on postoperative CT images, as described for the cadaveric study.

Follow-up Evaluation

Deviations in the coordinates of the entry and exit points on each dimension (x, y, z) were evaluated as described for the cadaveric study. The safety of the screw placement was evaluated in relation to vertebral canal perforation and graded as for the cadaveric study. Perioperative (2 weeks), short-term (3 months), and long-term (12 months) follow-up evaluations consisted of physical and neurological examinations. Neurological grading was only performed when dogs were assessed directly by veterinarians.

Statistical Analysis

For each vertebra, the mean deviations of the entry points or exit points between the planned coordinates and postoperative coordinates were obtained. The differences between the mean deviations of the entry points and those of the exit points were statistically compared for each dimension (x, y, z). Statistical analyses were performed using statistical software (JMP, SAS institute Japan, Inc., Tokyo, Japan). Data were presented as the mean ± standard deviation. A paired t-test was used for the analysis, specifying that $p < 0.05$ was considered statistically significant.

Results

Cadaveric Experimental Study

Twenty-two drill holes were made in cadaveric spinal specimens. In the accuracy evaluation of drill guide templates, the overall mean screw deviation was 0.88 ± 0.36 mm. The mean screw deviations at the entry and exit points were 0.81 ± 0.39 mm and 0.94 ± 0.32 mm, respectively. There were no statistically significant differences in the mean screw deviations (mm and percentages) of each vertebra between the entry points and exit points on each dimension (x, y, z) in cadaveric spinal specimens ($p > 0.05$) (Table 2-2). In the safety evaluation, exposure of the cortical bone was not observed and all drill holes were completely contained within the bone (i.e., grade 0).

Clinical Cases of Thoracolumbar Spinal Instability

On the basis of results of the cadaveric experimental study, spinal fixation was performed using the drill guide template system in clinical cases. Twenty-nine screws were placed in the thoracolumbar vertebrae of 4 cases. The accuracy of the screw locations in clinical cases was evaluated in a same manner to the cadaveric spinal specimens. The overall mean screw deviation was 1.16 ± 0.56 mm. The mean screw deviations at the entry and exit points were 0.85 ± 0.32 mm and 1.47 ± 0.58 mm, respectively. The mean deviations of the exit point were significantly larger in T11 and T12 than those of the entry point on the x axis ($p < 0.05$). The mean deviations of the exit point were significantly larger in T13 than those of the entry point on the x axis and y axis ($p < 0.05$) (Table 2-3).

In the safety evaluation, 26 out of 29 screws (89.6%) were located without evidence of vertebral canal exposure (grade 0 or 1). Screws on the cranial and caudal sides of T11 (case No.1) and on the caudal side of T13 (case No.3) perforated the wall of the bone structure (grade 1). Screws on the caudal side of T12 and on the cranial side of T13 (case No.3) perforated the wall of the bone structure (grade 2). One screw (3.45%) of L1 in case No.2 was located outside the bone (grade 3) (Table 2-4).

The results of the follow-up evaluations of these cases are summarized in Table 2-1.

Discussion

In the present study, I evaluated the accuracy and safety of the drill guide template system in cadaveric spinal specimens and clinical cases. The overall mean screw deviation was 0.88 ± 0.36 mm in cadaveric specimens. Penetration of the cortical bone was not observed and all drill holes were completely located in the bone. In clinical cases, the overall mean screw deviation was 1.16 ± 0.56 mm. In the safety evaluation, 26 out of 29 screws (89.6%) were placed without evidence of vertebral canal invasion. The deviation between the preoperative planned trajectories and postoperative screw corridors of the implants was small, and it was possible to place the implant accurately along pre-planned corridors. Using preoperative CT data, I designed and fabricated the drill guide templates so to avoid the injury to the large blood vessels. I have not encountered serious complications during surgery and through evaluation of the postoperative imaging and short and long-term follow-up. The excellent short and long-term clinical results in this study corroborate the safety of my patient-specific drill guide templates.

In the present study, 26 out of 29 (89.6%) screws were placed without evidence of vertebral canal invasion in clinical cases (Grade 0 and Grade 1). A possible reason for screw misdirection (Grade 2 and Grade 3) was that the drill sleeve angle had changed due to the load on the drill bit during the drilling procedure. This hypothesis was also supported by my observation that the mean screw deviations at the exit points were larger than those of the entry points. A three-step screw guide template system has been developed for a human spinal surgery in order to reduce the displacement of implants. This system consisted of 3 separate patient-specific lamina fit-and-lock templates and was validated for its accurate implant placement（55, 56, 105）. Another consideration is the materials of the drill guide template system. A flexible material that tightly fits the shape of the vertebral arch is suitable for the lamina cover, while a firm material may be appropriate for the drill sleeve, which resists the load during the drilling step.

Despite the possible risk of drill misdirection, intraoperative complications were not encountered in clinical cases. In the accuracy evaluation of drill guide templates in the cadaveric experimental study and clinical cases, the overall mean screw deviations were 0.88 ± 0.36 mm and 1.16 ± 0.56 mm, respectively. The greater accuracy observed in cadaveric specimens was most likely due to the more complete removal of soft tissues to which the drill guides were attached. Moreover, the operator was able to visually evaluate the entire spine, which may also have contributed to the greater accuracy of the drill guide template in cadavers. Although a critical breach of the canine thoracolumbar vertebrae has not yet been defined, we considered a deviation at the exit point exceeding 2.40 ± 1.06 mm (119.9 ± 53.08 %) to result in Grade 2 or Grade 3, thereby increasing the risk of implant failure and/or potential neurovascular injury. I also noted that greater accuracy was achieved for screws placed in the cranial lumbar vertebrae than those in the caudal thoracic vertebrae (Table 2-3). The placement of an implant in the caudal thoracic vertebrae is thought to be more demanding because it is placed in the vertebral body through the pedicle rather than directly in the vertebral body in the case of lumbar vertebrae.

The limitations of our drill guide template system include the need for the nearly complete removal of soft tissues from vertebrae in order to fit the template, which may compromise vascularization of the vertebra, the small number of dogs examined, the relatively short follow-up of clinical cases, and the lack of imaging follow-up. Although the references for veterinary patients/dogs about the cortical perforation percentages by freehand pedicle insertion are limited to the cervical vertebrae（21, 78） and not in the thoracolumbar vertebrae, comparison of the accuracy of my (SM) drill guide template system to that with freehand insertion on the incidence of complications should be performed. Additionally, stainless steel screws may have emphasized metal artifacts on postoperative CT scans, which may have been associated with inaccurate measurements of screw locations in clinical cases. I also wish to analyze the accuracy of the drill guide template in terms of a deviation of the screw trajectory in a three-dimensional manner in future study.

Tables and Figures

Table 2-1. Clinical information and findings of clinical cases

Case No.	Breed	Body weight (kg)	Sex	Clinical sign	Diagnosis	Lesion locations	Surgery	Neurological grade			
								Pre-surgery	Perioperative follow-up period, 2wks	Short follow-up period, 3 ms	Long follow-up period, 12 ms
1	Pug	7.1	SF	paraparesis	IVDD hypoplasia of posterior articular	T11-12 T12-13	corpectomy vertebral fixation	3a	3a	4	4
2	Pug	7.8	CM	paraparesis	IVDD hypoplasia of posterior articular	T11-12 T12-13 T13-L1	mini-hemilaminectomy corpectomy vertebral fixation	3a	4	4	4
3	Pug	4.75	SF	paraparesis	IVDD aplasia of posterior articular	T12-13 T13-L1 L1-2	mini-hemilaminectomy vertebral fixation	3a	4	4	4
4	American Cocker Spaniel	10.3	M	paraparesis	IVDD spondylosis deformans	T13-L1 L1-2 L2-3 L3-4	mini-hemilaminectomy vertebral fixation	3a	4	4	4

Neurological grades were defined based on Modified Frankel Score; 5, Normal gait with paraspinal hyperesthesia; 4, Ambulatory paraparesis; 3a, Nonambulatory paraparesis (ability to bear weight on the pelvic limbs without support); 3b, Nonambulatory paraparesis (inability to bear weight on the pelvic limbs without support); 2, Paraplegia with intact nociception; 1, Paraplegia with absent superficial nociception; 0, Paraplegia with absent deep nociception. SF, spayed female; F, intact female; CM, castrated male; M, intact male; wks, weeks; ms, months.

Table 2-2. Accuracy of screw locations with drill guide templates for cadaveric spines

Spine	Entry point				Exit point		
	x	y	z		x	y	z
T12, mm	0.45 ± 0.29	0.82 ± 0.56	0.79 ± 0.36		0.68 ± 0.50	0.67± 0.39	1.62 ± 0.85
T12, %	22.45 ± 14.72	40.83 ± 27.99	39.56 ± 17.94		33.92 ± 25.10	33.23 ± 19.29	80.98 ± 42.40
T13, mm	0.52 ± 0.34	0.81 ± 0.44	1.35 ± 0.85		1.18 ± 1.04	0.53 ± 0.20	1.31± 0.74
T13, %	26.13 ± 17.00	40.30 ± 22.18	67.97 ± 42.23		58.93 ± 51.94	26.37 ± 9.85	65.38 ± 37.08
L1, mm	0.44 ± 0.25	0.67 ± 0.62	0.73 ± 0.63		0.93 ± 0.58	0.96 ± 0.74	1.04 ± 0.85
L1, %	21.87 ± 12.32	33.47 ± 31.06	36.59 ± 31.59		46.63 ± 29.13	48.23 ± 37.02	51.75 ± 42.64

Comparisons of the mean screw deviations of each vertebra of cadaveric spinal specimens of the entry and exit points on each dimension (x, y, z) before and after surgery between the entry points on each dimension and the exit points on each dimension. *$p < 0.05$

Table 2-3. Accuracy of screw locations with drill guide templates for clinical cases

Spine	Entry point			Exit point		
	x	y	z	x	y	z
T11, mm	0.73 ± 0.16	0.84 ± 0.16	1.76 ± 0.98	3.19 ± 0.89*	1.27 ± 0.82	1.83 ± 0.79
T11, %	36.48 ± 8.01	41.74 ± 7.86	87.90 ± 48.79	159.63 ± 44.55*	63.56 ± 41.09	91.48 ± 39.47
T12, mm	0.44 ± 0.14	0.37 ± 0.19	0.97 ± 0.48	2.62 ± 1.36*	0.66 ± 0.27	1.45 ± 1.63
T12, %	22.89 ± 7.16	18.93 ± 9.7	48.98 ± 24.06	154.65 ± 67.96*	28.20 ± 13.62	90.48 ± 81.54
T13, mm	0.44 ± 0.28	1.21 ± 0.62	0.59 ± 0.58	2.40 ± 1.26*	0.79 ± 0.55*	1.04 ± 0.95
T13, %	21.81 ± 13.95	60.46 ± 30.90	29.29 ± 29.18	119.99 ± 62.89*	39.36 ± 27.43*	52.45 ± 47.51
L1, mm	0.44 ± 0.63	0.73 ± 1.02	0.86 ± 1.08	2.50 ± 3.72	0.51 ± 0.85	0.92 ± 1.09
L1, %	21.84 ± 7.36	36.59 ± 26.53	43.23 ± 29.84	125.08 ± 161.45	25.44 ± 18.08	45.93 ± 30.17
L2, mm	0.36 ± 1.04	0.79 ± 1.21	1.17 ± 1.45	1.39 ± 1.66	0.77 ± 1.13	1.44 ± 1.69
L2, %	17.99 ± 15.71	39.51 ± 24.04	58.54 ± 35.92	69.68 ± 46.47	38.28 ± 20.19	71.83 ± 47.92
L3, mm	0.48 ± 1.37	0.86 ± 1.73	2.26 ± 1.46	0.74 ± 1.71	0.39 ± 1.28	2.53 ± 1.22
L3, %	24.13 ± 9.38	42.83 ± 27.08	112.75 ± 13.96	37.08 ± 26.48	19.58 ± 4.58	126.25 ± 1.96

Comparisons of the mean screw deviations of each vertebra of clinical cases of the entry and exit points on each dimension (x, y, z) before and after surgery between the entry points on each dimension and the exit points on each dimension. *$p < 0.05$

Table 2-4. Safety of screw insertion with drill guide templates for clinical cases

Grade	Number of Screws						Safety (%)
	T11	T12	T13	L1	L2	L3	
Grade0	2	4	6	5	4	2	23/29 (79.3)
Grade1	2	0	1	0	0	0	3/29 (10.3)
Grade2	0	1	1	0	0	0	2/29 (6.9)
Grade3	0	0	0	1	0	0	1/29 (3.5)
Total	4	5	8	6	4	2	29/29 (100)

Grading of the screw trajectory was as follows: Grade 0 (containing), Grade 1 (exposure), Grade 2 (perforation), and Grade 3 (penetration).

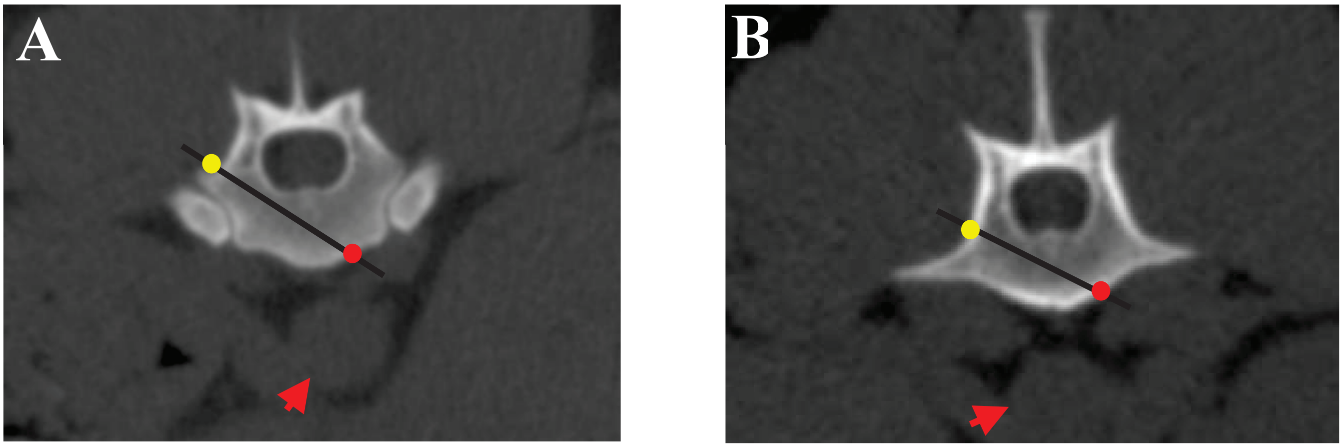

Figure 2-1. Determination of the optimum screw trajectories

Cranial of T12 (A). Caudal of L1 (B). Optimum screw trajectories were selected for the thoracolumbar vertebrae (T12-L1). The ideal trajectories and their coordinates of the bone entry and exit points were determined, and 6 trajectories were selected for T12-L1 (2 trajectories for each vertebra). Solid yellow circles indicate entry point of the drilling, and solid red circles indicate exit point of the drilling. White lines indicate optimum screw trajectories. Red arrows indicate the abdominal aorta.

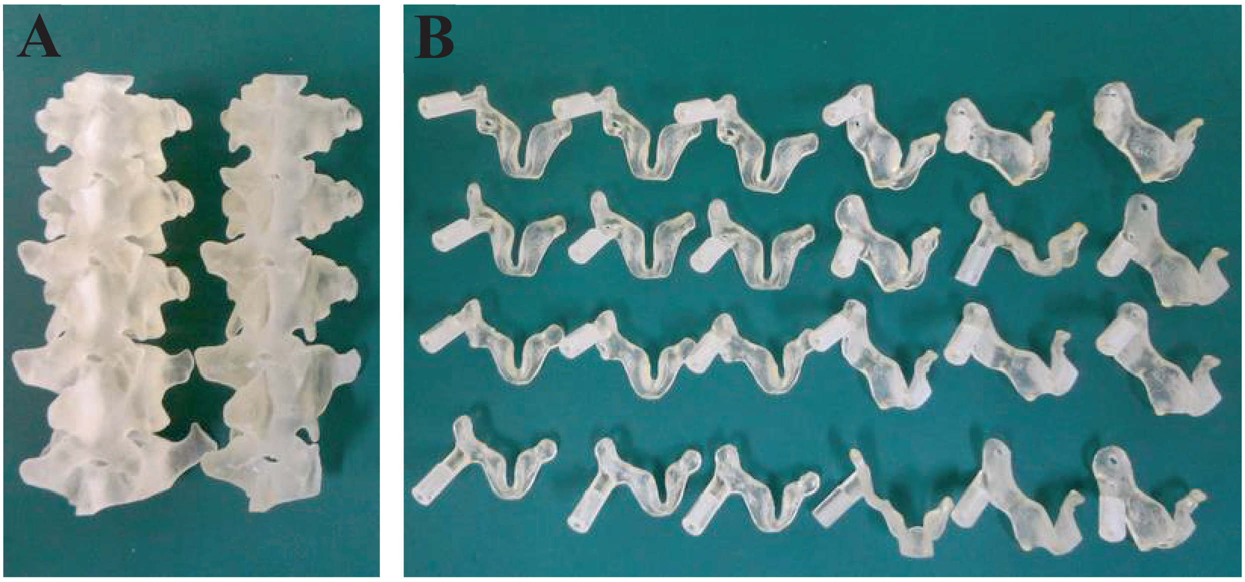

Figure 2-2. The patient-specific bone models and drill guide templates

Three-dimensional-printed thoracolumbar vertebrae (T11-L1) (A) and the corresponding 3-dimentional patient-specific drill guide templates (B).

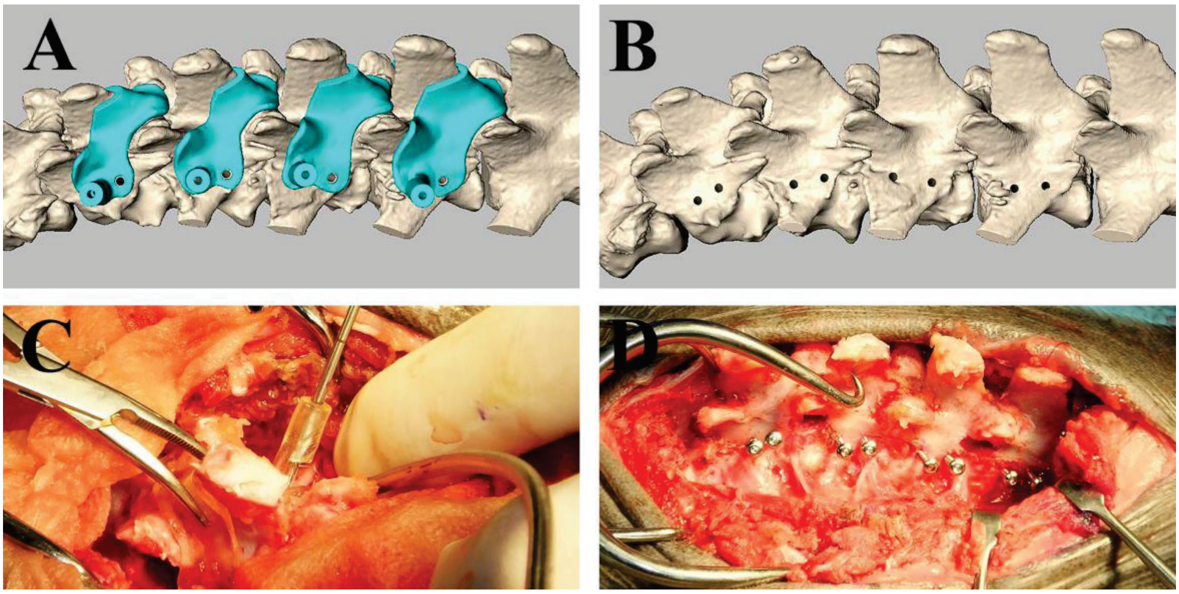

Figure 2-3. Design of the drill guide templates and placement of the screws

Drill guide templates comprised 1.5-mm-wide cylindrical sleeves extending from the platform that fits the patient-specific 3-dimentional shape of the lamina (A). In each case, a simulation of screw hole placement was confirmed (B). Drill guide templates were firmly attached to the lamina, and screw holes (bi-cortical) were made with a drill bit (C, D). One to 2 screws were placed in each vertebral body.

Chapter 3

Accuracy and efficacy of a patient-specific drill guide template system for lumbosacral junction fixation in medium and small dogs: cadaveric study and clinical cases.

Introduction

Lumbosacral luxation in dogs caused by DLSS, trauma (fracture and/or luxation), discospondylitis, neoplasia. DLSS is characterized by stenosis of the spinal canal, causing compression of the cauda equina in dogs. Although this condition is most commonly seen in medium- and large-sized dogs, it can also be seen in small dogs, typically presenting with caudal lumbar back pain（108）.

Surgical treatment for DLSS is the standard choice of treatment in the presence of severe caudal lumbar pain or neurologic deficits that do not respond to conservative therapies（100, 106）. The reported surgical techniques for DLSS include dorsal laminectomy alone or in combination with partial discectomy, dorsal laminectomy combined with fixation and fusion, or lateral foraminotomy（33, 34, 37, 68, 98, 100）. Although the reported rate of short-term improvement of clinical signs with decompressive surgery is as high as 78-93%（27, 108）, the long-term recurrence rate of clinical symptoms is also relatively high at 17-38%（27, 108）. Decompressive surgery alone could further aggravate instability of the lumbosacral junction, and dorsal vertebral body fixation should therefore be considered in cases with a high risk of postoperative instability at the surgical site（27, 98, 106）.

Fixation of the lumbosacral junction is commonly achieved by implants, such as pins and/or screws, placed within the pedicles or vertebral bodies along with PMMA（33, 76, 118）, or by using a pedicle screw-rod fixation system（68, 108, 109, 127）. The advantage of dorsal fixation is that it provides stability to the lumbosacral junction and can reduce dynamic compression of the spinal cord

（34, 68, 108）. However, the placement of implants for lumbosacral junction fixation carries a potential risk of iatrogenic injury to vital structures including cauda equine, nerve roots and vasculature（100）. The accurate placement of implants is thus of upmost importance to achieve rigid fixation and also to avoid injury to the surrounding anatomy. Although the optimal implant trajectory for lumbosacral fixation has been reported（100）, freehand insertion of implants is widely performed in specialty between veterinary and practice, which is oftentimes problematic for placing the implants in the ideal trajectory. In addition, the freehand technique carries an increased risk of complications, such as iatrogenic injury of cauda equine, nerve roots and vasculature, together with insufficient stability due to a lack of rigid attachment to the vertebrae and complete biologically fusion.

In Chapter 2, I reported a patient-specific drill guide template, which was developed as an inexpensive device to accurately guide spinal fixation screws in the thoracolumbar vertebrae of dogs. In Chapter 3, I assessed the accuracy of patient-specific drill guide templates for screw placement in the lumbosacral junctions, which has a different shape from the thoracolumbar spine and stabilized by bilateral transarticular facet screws. I applied this system to 6 canine cadavers and 3 clinical cases with lumbosacral luxation.

Materials and Methods

Cadaveric Study

All procedures were performed in accordance with the guidelines regulating animal use and ethics at Gifu University (approval number: 17211). The caudal lumbar spine (L6-7) and sacrum were removed from 6 cadavers of adult beagles that were used in other research projects and euthanized for reasons unrelated to the present study. The median age was 36 months (range: 20-54 years). The median body weight was 10 kg (range: 9-11.9 kg). All epaxial muscles were left intact. The spinal specimens were wrapped in saline (0.9% NaCl) solution-soaked paper towels and stored at -20°C until use.

Determination of Screw Trajectories

CT scanner (Alexion Advance, Canon Medical System Corporation, Tochigi, Japan) was used to obtain 0.5 mm-slice preoperative images of the caudal lumbar and sacrum region. The images obtained by CT imaging were exported to 3D / multiplane imaging software (Ziostation, Ziosoft, Tokyo, Japan) in the DICOM format. I then selected the optimal implant trajectories for L7, the L7-S articular processes, and the sacrum using MPR images. The entry point of the L7 implant was at the base of each dorsal articular process. In the L7-S articular facet, I planned drill trajectories in order to place the implant through the caudal articular process of L7 and the cranial articular surface of the sacrum. Specifically, the trajectories were planned such that the angle of the screw was 30-45° in the sagittal plane and 45-60° in the transverse plane, extending from the dorsomedial surface of L7 to the ventrolateral surface of the sacrum. The entry point of the sacrum screw was cranial aspect of sacrum, medial to the caudal articulation of L7 and the sacrum. The trajectories were planned so as to avoid injury to surrounding important structures such as the cauda equina, nerve roots, and blood vessels. The 3D coordinates of the entry points and exit points on L7, the articular processes, and the sacrum were subsequently recorded and used to design the drill guide templates (Figure 3-1).

Design and Fabrication of Patient-Specific Drill Guide Templates

I designed and fabricated the drill guide templates as I reported in Chapter 2. Briefly, bone processing data were extracted from the DICOM data using image processing software (VG Studio Max, Volume Graphics GmbH, Heidelberg, Germany and Mimics, Materialize, Leuven, Belgium) and transferred to 3D modeling software (Freeform, Data Design, Nagoya, Japan) to generate a 3D reconstruction model. Using a 3D printing system (Connex500, Stratasys, Tokyo, Japan), patient-specific drill guide templates were fabricated from non-soluble acryl. The drill guide template consisted of a cylindrical sleeve (inner diameter of 1.5 mm) and a platform to fit the patient-specific 3D shape of the L7 vertebral arch and sacrum (Figure 3-2). I also made a patient-specific 3D bone model to confirm the fit of the templates and the angle of the drill sleeve in relation to the vertebral body before surgery. The drill guide templates and bone models were sterilized with ethylene oxide gas before surgery.

Drilling of Cadaveric Vertebrae Using Drill Guide templates

Before drilling, the specimens of the caudal lumbar spine (L6-7) and sacrum were thawed in warm water. The spinous process and vertebral arch were exposed by dissecting paraxial muscle tissues from the specimens. Drill guide templates were firmly attached to the lamina by curved Halsted mosquito forceps, and bi-cortical screw holes were made with a drill bit (1.5 mm) (Figure 3-3). The locations of the drill holes were examined on postoperative CT images.

Evaluation of The Accuracy and Safety of Drill Guide Templates

To estimate deviations of the screw trajectories, we made fusion images of the preoperative and postoperative CT images. DICOM data were imported into 3D / multiplane imaging software (Ziostation, Ziosoft, Tokyo, Japan), and six landmarks were registered on the postoperative MPR images. The landmarks used were the spinous process, transverse process, and intervertebral foramina for L7, and the intermediate sacral crest, the median sacral crest, and dorsal sacral foramina for the sacrum. Subsequently, fusion images were made by superimposing the postoperative MPR image on the preoperative MPR image, and the coordinates of the entry and exit points of the drill holes on the fusion images were recorded (Figure 3-4). Deviations in the coordinates of the entry and exit points in each dimension (x, y, z) were evaluated, as in Chapter 2. To evaluate the safety of the drill guide templates, drill hole displacement was graded using postoperative transverse and sagittal CT images as a reference. Grading of the drill hole trajectories was as follows: Grade 0 (containing) - the drill hole trajectory was completely within the wall of the bone structure; Grade 1 (exposure) - the drill hole trajectory invaded the wall of the bone structure, while more than 50% of the drill hole diameter remained within the bone; Grade 2 (perforation) - the drill hole trajectory invaded the bone structure and more than 50% of the drill hole diameter was outside the bone structure; Grade 3 (penetration) - the drill hole trajectory completely penetrated outside the bone structure（55, 70, 124）.

Clinical Cases

Imaging studies and surgical procedures were performed at the Animal Medical Center of Gifu University with the informed consent of the owners. I performed surgical stabilization using drill guide templates in three clinical cases. I performed neurological examinations, CT imaging, and MRI (0.4-Tesla APERTO Eterna, Hitachi Healthcare, Tokyo, Japan). The neurological status of each dog was classified using MFS. All three cases were diagnosed as luxation of the lumbosacral junction. One case showed chronic progressive paraparesis and ataxia, which were thought to result from spinal instability based on imaging findings of degenerative changes, such as IVD degeneration, and spondylosis deformans（27, 29, 34, 69, 121）. The other two cases were diagnosed as spinal instability due to trauma, based on imaging findings of lumbosacral luxation. Clinical information and imaging findings of the three cases are summarized in Table 3-1.

Surgeries

Case 1

Based on clinical finding and advanced imaging, dorsal laminectomy with partial discectomy was performed to decompress the cauda equina. After releasing the epaxial musculature from the spinous processes, articular processes, lamina arch of L7, and sacrum, the drill guide template was firmly attached to the caudal articular processes with Adson tweezers. A 0.9-mm pin (0.035" miniature half-pin, IMEX Veterinary, Inc., Texas, USA) was then inserted into the cylinder sleeve and a drill hole was made while visually confirming the entry point from the opening of the drill sleeve. Subsequently, the depth of the drill hole was measured using a depth gauge, the length of the drill hole was evaluated, and bilateral transarticular facet screws (M 2.0 cortical bone screw, Mizuho, Tokyo, Japan) with a diameter of 2 mm were placed. Postoperative CT imaging was performed (Figure 3-5).

Case 2

After skin incision, the epaxial musculature was released from the vertebral body, and the luxation of the lumbosacral junction was reduced by pulling the spinous process of L7 and the median sacral crest with bone holding forceps or towel forceps while confirming the alignment of the L7-S under fluoroscopy. Screws were placed using the drill guide template; two screws were placed in each of the L7, L7-S articular facets, and sacrum. The head of the screw was exposed 10 mm from the lamina surface for bone cement engagement. Bone cement (Surgical Simplex P, Stryker, Tokyo, Japan) was applied in order to cover the screw heads. The locations of the screws were examined on postoperative CT images.

Case 3

A dorsal median incision was performed from the spinous process of L6 to the sacrum. After the epaxial musculature was released from the vertebrae, a thickened ligamentum flavum was observed between the L7 and sacrum, which was removed with dissecting forceps. The luxation of the lumbosacral junction was reduced by pulling the spinous process of L6 to the sacrum with small serrated bone holding forceps or Backhaus towel forceps. After the drill guide template was attached to the L7 and sacrum, a 0.9-mm pin was then inserted into the cylinder sleeve. After inserting the pin, CT imaging was performed to confirm the drilled trajectory, the pin was removed, tapping of the drill hole was performed, and two screws were placed in each of the L7 with the base of each dorsal articular process and sacrum. After the placement of screws, dorsal laminectomy was performed, and bone cement was applied in the same manner as for Case 2. The locations of the screws were examined on postoperative CT images (Figure 3-6).

Follow-up Evaluation

Postoperative (2 weeks) follow-up evaluations consisted of physical and neurological examinations. Neurological grading was only performed when dogs were assessed directly by veterinarians. I also confirmed the clinical progress at one year after surgery by telephone interview or physical examination.

Statistical Analysis

For each vertebra, deviations in millimeters between the planned coordinates and the actual coordinates were obtained. The differences between the mean deviations of the entry points and those of the exit points were statistically compared for each dimension (x, y, z) using statistical software (JMP, SAS institute Japan, Inc., Tokyo, Japan). Data were presented as the mean ± standard deviation. A paired t-test was used for the analysis, with significance set at $p < 0.05$.

Results

Cadaveric Study

Thirty-six drill holes were made in the cadaveric spinal specimens. In comparison to the planned trajectory, the mean drill hole deviations of the drilled trajectory at the entry and exit points were 1.52 ± 0.77 mm and 2.57 ± 1.53 mm, respectively. The mean deviations of the exit point were significantly larger in L7-S1 (right) than those of the entry point on the x axis and y axis ($p < 0.05$). The mean deviations of the exit point were significantly larger in L7-S1 (left) than those of the entry point on the z axis ($p < 0.05$) (Table 3-2). In the safety evaluation, I made 12 pedicle screws in L7 and 12 drill holes for transarticular screws. In addition, 12 screw holes were made in the dorsal aspect of the sacrum, medial to the cranial articular surface of the sacrum in a pedicle screw fashion. Exposure of the drill holes from the cortical bone was not observed, and all drill holes were completely contained within the bone (i.e., Grade 0).

Clinical Cases

A total of twelve screws (4 pedicle screws in L7, 4 screws placed in the dorsal aspect of sacrum and 4 transarticular screws) were placed in the L7, L7-S articular facet, and the sacrum in three clinical cases. The accuracy of the screw locations in clinical cases was evaluated in the same manner as for the cadaveric spinal specimens. The mean drill hole deviations at the entry and exit points were 1.95 ± 0.93 mm and 2.91 ± 1.01 mm, respectively. There were no statistically significant differences in the mean screw deviations (mm and percentages) of each vertebra between the entry points and exit points on each dimension (x, y, z) in cadaveric spinal specimens (Table 3-3). In the safety evaluation, I made 4 pedicle screws in L7, 4 screws placed in the dorsal aspect of sacrum and 4 transarticular screws. Exposure of the screws from the cortical bone was not observed, and all drill holes were completely contained within the bone (i.e., Grade 0). After surgery, the motor function of clinical cases recovered and back pain was resolved within 2 weeks. For case 2, I confirmed by telephone interview that the clinical status was good for more than one year after surgery. The results of the follow-up evaluations of the three cases are summarized in Table 3-1.

Discussion

In the present study, I evaluated the accuracy and safety of the drill guide template system in cadaveric spinal specimens and clinical cases. The main finding of the present study was that cortical bone was not exposed, as all drill holes were completely located within the bone in both cadaveric spinal specimens and clinical cases. The drill guide template system allowed safe placement of 12 pedicle screws in L7, 12 screw holes in the dorsal aspect of the sacrum and 12 drill holes for transarticular screws in the cadaveric study, and 4 pedicle screws in L7, 4 screws placed in the dorsal aspect of sacrum and 4 transarticular screws in clinical cases. I designed and fabricated the drill guide templates, using preoperative CT data, to avoid penetration of the screws to the spinal canal. I encountered no serious complications during surgery or perioperative follow-up period in the three clinical cases. These results corroborate the safety of our patient-specific drill guide templates designed for lumbosacral fixation surgery.

The mean deviations of the exit points were significantly larger than those of the entry points in the cadaveric spine specimens. Additionally, the mean deviations of the exit point were significantly larger in L7-S1 than those of the entry point in the cadaveric study. The cause of this deviation of the drilled holes was thought that the angle of the drill sleeve of the drill guide template or the position of the platform changed due to the load in the medial-lateral, ventral-dorsal and craniocaudal direction during the drilling procedure. Another cause of deviation was considered to be associated with transarticular drill holes in L7 - S1. I thus need to consider countermeasures for drill misdirection when using my drill guide template system. In order to reduce displacement of the implant, a three-step screw guide template system has been developed for human spinal surgery（55, 105）. This system has been verified for accurate implant implantation and shows favorable clinical outcomes in small dogs. I think that it is feasible to further reduce deviation with reference to this system. 3D shape of the drill guide templates ensures that the procedure cannot be affected by spinal alignment changes, such as torsion during drilling and screw placement. In addition, I need to optimize the material of the drill guide template system to reduce deviation. A flexible material that fits tightly to the contour of the vertebral arch is suitable for the lamina cover, while a firm material that resists the load during drilling may be more suitable for the drill sleeve. I think about the material of the drill guide template as follows. The lamina cover of drill guide template is fabricated of a flexible silicone material that fits tightly the vertebral arch, and the drill sleeve should be fabricated of a hard acrylic material that is resistant to loads. Although the deviation between the preoperative planned trajectories and drilled trajectories in this study was larger than that of the thoracolumbar vertebrae in chapter 2, all drill holes were completely located within the bone, and no intraoperative complications were experienced in the clinical cases.

Limitations of the present study include the small number of clinical cases, short follow-up periods of clinical cases, lack a control group, and the lack of an imaging study at follow-up. Regarding the placement of the implants in the lumbosacral vertebrae, there has been no report on the percentages of cortical perforation by freehand pedicle screw insertion in veterinary medicine, and I was thus unable to compare the accuracy of my drill guide template system with that of freehand insertion and the incidence of complications between these techniques. Therefore, when assessing the accuracy of the drill guide templates, I created surgical fusion images by superimposing the postoperative MPR image on the preoperative MPR image. The stainless-steel screws may have caused metal artifacts on postoperative CT scans, and this may have resulted in incorrect measurement of the screw positions in the clinical cases. Although two-dimensional analysis was performed on the displacement of screw locations, I would like to analyze the accuracy of the drill guide template in a 3D study in the future.

Tables and Figures

Table 3-1. Clinical information and findings of clinical cases

Case No.	Breed	Body weight (kg)	Age(months)	Sex	Clinical sign	Diagnosis	Surgery	Screw location	Follow-up period	Neurological grade		
										Pre-surgery	Perioperative follow-up	Last follow-up period
1	Toy poodle	4.1	96	SF	paraparesis, caudal lumbar pain, pelvic limb lameness	lumbosacral subluxation, discospondylitis	dorsal laminectomy, partial disectomy, transarticular facet fixation	L7-S1	12	3a	4	4
2	Yorkshire terrier	2.9	84	F	caudal lumbar pain	lumbosacral luxation	L7-S1 screw-PMMA fixation	L7-S1	7	3a	4	4
2	Toy poodle	4.2	88	M	caudal lumbar pain	lumbosacral luxation	L7-S1 screw-PMMA fixation	L7-S1	1	5	5	5

Neurological grades were defined based on Modified Frankel Score: 5, Normal gait with paraspinal hyperesthesia; 4, Ambulatory paraparesis; 3a, Nonambulatory paraparesis (ability to bear weight on the pelvic limbs without support); 3b, Nonambulatory paraparesis (inability to bear weight on the pelvic limbs without support); 2, Paraplegia with intact nociception; 1, Paraplegia with absent superficial nociception; 0, Paraplegia with absent deep nociception. SF, spayed female; F, intact female; M, intact male.

Table 3-2. Accuracy of drill hole locations with drill guide templates for cadaveric spines

Spine	Entry point				Exit point		
	x	y	z		x	y	z
L7(L), mm	0.41 ± 0.10	0.50 ± 0.48	0.88 ± 1.08		0.37 ± 0.21	0.59 ± 0.37	2.64 ± 1.65
L7(L), %	20.33 ± 4.99	25.08 ± 24.23	43.83 ± 54.24		18.58 ± 10.72	29.42 ± 18.27	131.92 ± 82.36
L7(R), mm	0.30 ± 0.18	0.78 ± 0.50	0.86 ± 0.62		0.38 ± 0.33	1.09 ± 0.60	2.05 ± 1.51
L7(R), %	15.00 ± 9.03	38.83 ± 24.84	43.08 ± 30.38		18.83 ± 16.54	54.25 ± 30.07	102.42 ± 75.48
L7-S1(L), mm	0.88 ± 0.73	0.60 ± 0.43	0.76 ± 0.42		1.80 ± 1.48	1.05 ± 0.99	2.07 ± 1.07*
L7-S1(L), %	44.0 ± 36.73	30.00 ± 21.29	38.08 ± 20.86		89.92 ± 73.98	52.33 ± 49.56	103.58 ± 53.65*
L7-S1(R), mm	0.73 ± 0.37	0.31 ± 0.47	1.41 ± 0.88		1.57 ± 0.92*	1.15 ± 0.77*	2.48 ± 2.07
L7-S1(R), %	36.67 ± 18.53	15.25 ± 23.27	70.67 ± 43.76		78.67 ± 45.94*	57.42 ± 38.71*	124.17 ± 103.34
S1(L), mm	0.46 ± 0.31	0.66 ± 0.32	0.84 ± 0.61		0.68 ± 0.56	0.61 ± 0.34	0.88 ± 0.46
S1(L), %	22.83 ± 15.75	32.75 ± 15.82	42.17 ± 30.34		33.75 ± 27.81	30.58 ± 16.95	43.83 ± 22.90
S1(R), mm	0.38 ± 0.42	0.91 ± 0.77	1.59 ± 0.44		0.82 ± 0.71	0.71 ± 0.37	1.23 ± 0.94
S1(R), %	19.08 ± 21.21	45.67 ± 38.60	79.50 ± 22.24		41.08 ± 35.72	35.67 ± 18.55	61.33 ± 46.84

Comparisons of the mean screw deviations of each vertebra of cadaveric spinal specimens of the entry and exit points on each dimension (x, y, z) before and after surgery between the entry points on each dimension and the exit points on each dimension. *$p < 0.05$

Table 3-3. Accuracy of screw locations with drill guide templates for clinical cases

Spine	Entry point				Exit point		
	x	y	z		x	y	z
L7(L), mm	0.45 ± 0.21	0.59 ± 0.09	1.02 ± 0.92		0.51 ± 0.40	2.00 ± 1.30	2.41 ± 0.91
L7(L), %	22.52 ± 10.68	29.68 ± 4.68	50.85 ± 46.1		25.30 ± 19.95	100.60 ± 65.40	120.25 ± 45.55
L7(R), mm	0.48 ± 0.48	1.40 ± 0.50	0.89 ± 0.48		1.27 ± 0.76	0.41 ± 0.27	2.70 ± 0.42
L7(R), %	24.20 ± 24.00	69.85 ± 25.00	44.55 ± 24.20		63.63 ± 38.08	20.60 ± 13.65	135.00 ± 21.10
L7-S1(L), mm	0.76 ± 0.49	0.46 ± 0.32	3.02 ± 0.15		0.98 ± 0.41	0.92 ± 0.01	1.71 ± 1.69
L7-S1(L), %	37.88 ± 24.48	23.13 ± 16.18	151.22 ± 7.53		48.80 ± 20.40	45.75 ± 0.70	85.72 ± 84.68
L7-S1(R), mm	1.32 ± 0.74	0.27 ± 0.12	2.45 ± 0.64		1.49 ± 0.23	1.26 ± 0.23	2.71 ± 0.59
L7-S1(R), %	65.95 ± 36.80	13.25 ± 6.15	122.35 ± 32.15		74.25 ± 11.55	62.93 ± 42.58	135.40 ± 29.50
S1(L), mm	1.06 ± 0.19	1.02 ± 0.21	0.34 ± 0.11		0.66 ± 0.42	1.46 ± 0.03	2.24 ± 0.93
S1(L), %	52.88 ± 9.58	50.83 ± 10.73	17.20 ± 5.35		32.80 ± 20.80	73.23 ± 1.38	112.05 ± 46.40
S1(R), mm	0.10 ± 0.05	0.36 ± 0.01	0.54 ± 0.14		0.31 ± 0.01	1.16 ± 0.13	1.00 ± 0.09
S1(R), %	5.05 ± 0.53	18.03 ± 0.53	27.20 ± 7.15		15.40 ± 35.72	58.00 ± 6.50	50.20 ± 4.70

Comparisons of the mean screw deviations of each vertebra of clinical cases of the entry and exit points on each dimension (x, y, z) before and after surgery between the entry points on each dimension and the exit points on each dimension. *$p < 0.05$

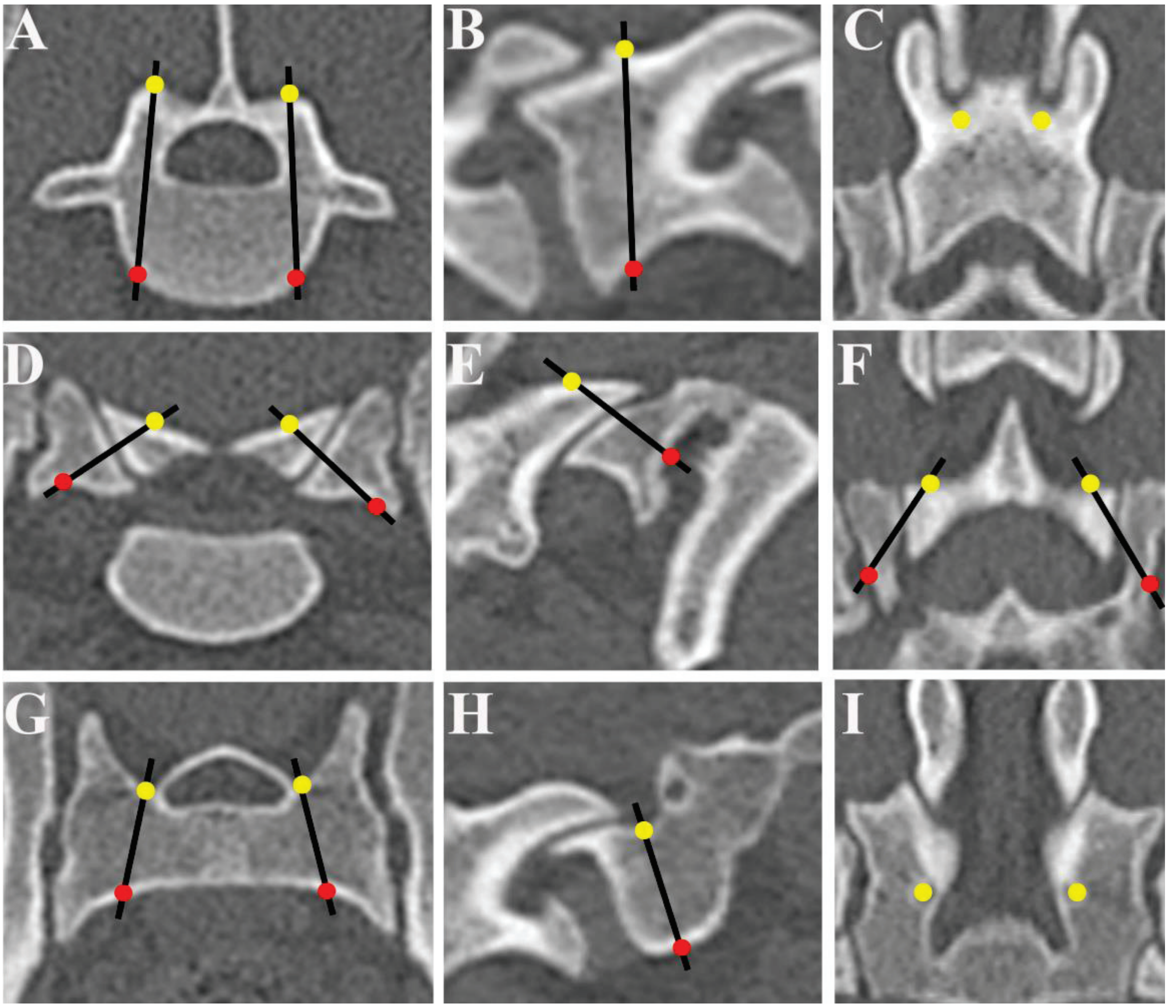

Figure 3-1. Determination of optimum screw trajectories

The trajectories and the coordinates of the bone entry and exit points were determined and six trajectories were selected for L7 on the transverse plane (A), sagittal plane (B), and dorsal plane (C), for L7-S1 articular processes on the transverse plane (D), sagittal plane (E), and dorsal plane (F), and for the sacrum on the transverse plane (G), sagittal plane (H), and dorsal plane (I). The entry points of the drilling holes are indicated by solid yellow circles and the exit points by solid red circles. The optimum screw trajectories are indicated by black lines.

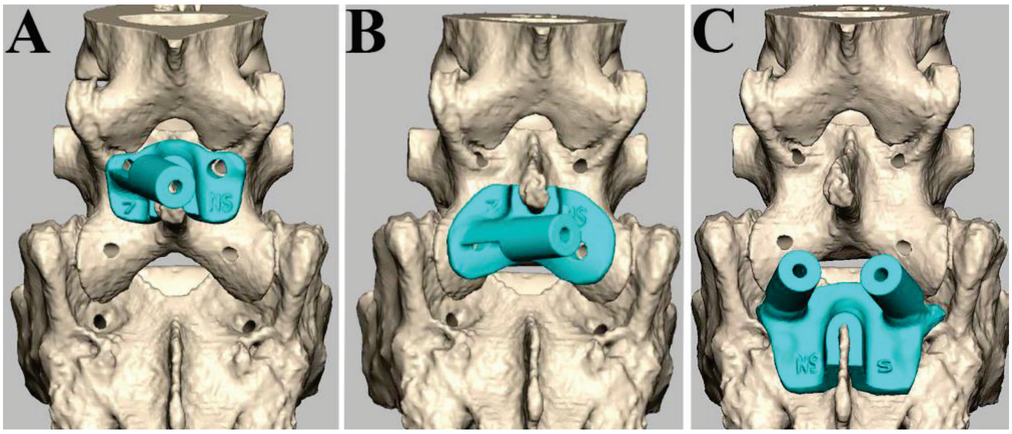

Figure 3-2. Design of patient-specific drill guide templates

The drill guide template for the left side of L7 (A), the left articular process (B), and both sides of S1 (C).

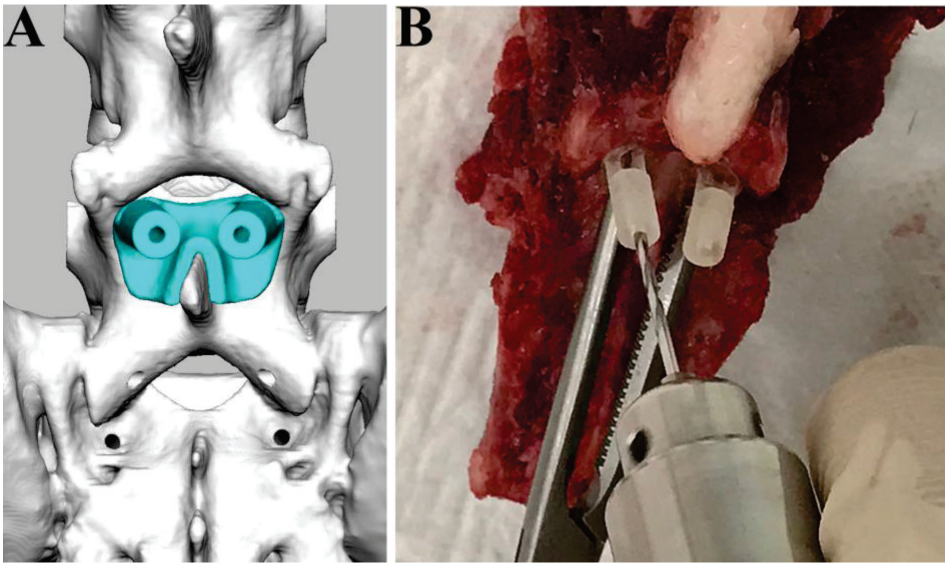

Figure 3-3. Drilling procedure for L7 using drill guide templates.

The drill guide template for L7 was designed (A) and applied for the cadaveric spine (B).

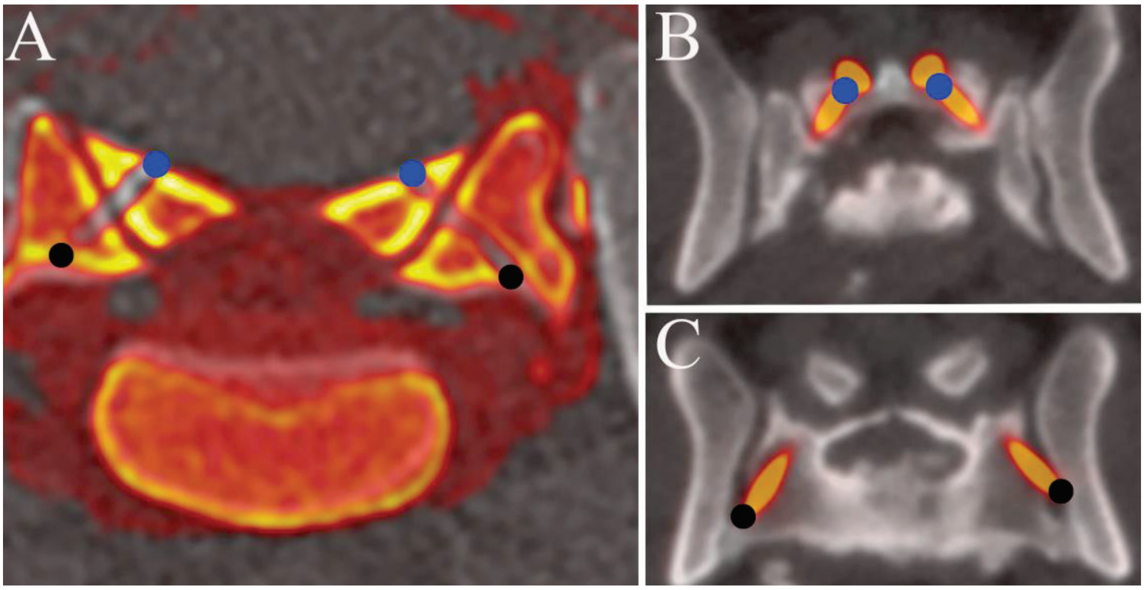

Figure 3-4. Fusion images of pre and postoperative MPR images of the L7-S1 articular processes. (A) Cadaveric study. (B,C) Clinical case (Case 1)

The coordinates of the entry and exit points obtained with the fusion image were compared with those planned before surgery. The entry points of the drill holes or screws are indicated by solid blue circles and the exit points by solid black circles.

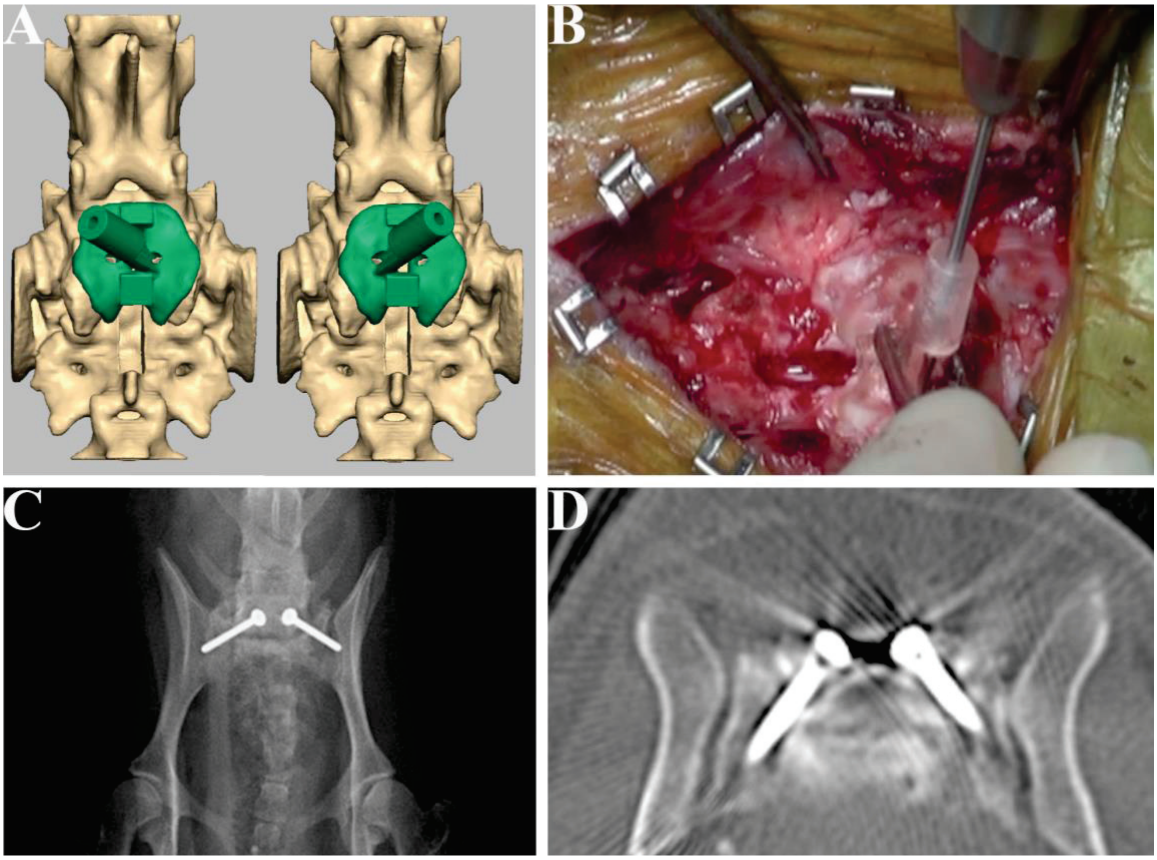

Figure 3-5. Design of the drill guide templates and placement of the screws for Case 1

Drill guide templates were designed for the articular facet (A) and were used at the drilling step (B). Postoperative radiograph (C) and CT image (D) of the lumbosacral junction.

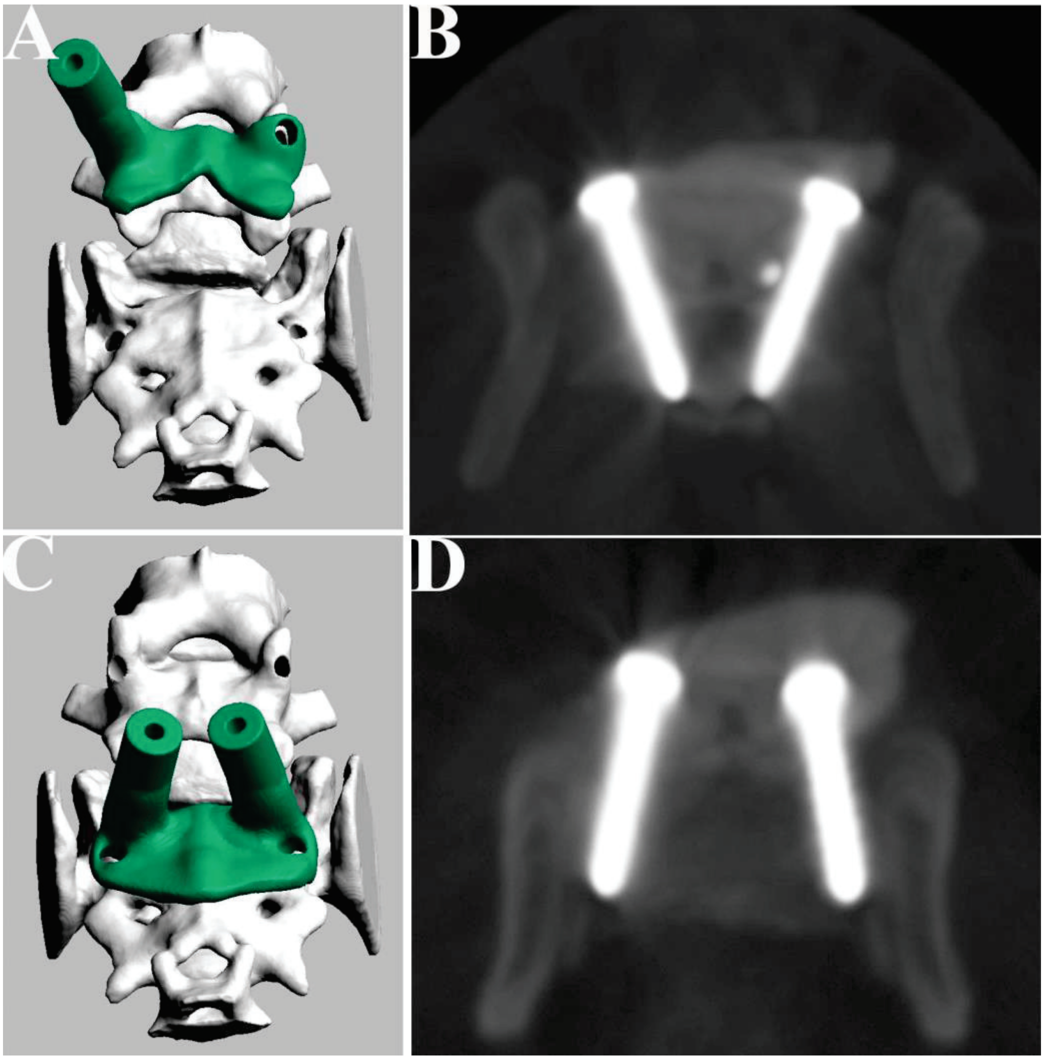

Figure 3-6. Design of the drill guide templates and placement of the screws for Case 2

Drill guide templates were designed for L7 (A) and sacrum (C). Postoperative CT image of the L7 (B) and sacrum (D).

Chapter 4

Conclusion

For canine cervical spine instability, distraction-stabilization techniques using intervertebral spacers and locking plates (mono-cortical screw placement) have recently been reported in place of bi-cortical implant placement in combination with PMMA in a small number of clinical cases. The evaluation of the efficacy of these distraction- stabilization techniques has mostly been based on clinical findings and follow-up imaging, however quantitative analyses of the degree of distraction have not been reported. Additionally, the distraction-stabilization technique may lead to loss of vertebral distraction before bony fusion. In Chapter 1 of my dissertation, I morphometrically analyzed the effect of vertebral distraction and evaluated the degree of decompression of the spinal cord after insertion of the intervertebral spacer and assessed the effects of the distraction and fusion technique based on clinical and imaging findings. The mean follow-up period was 18.8 months (range, 12-34 months). The neurologic scores were improved post-surgery in 6/6 dogs. Bridging new bone around the spacer was confirmed by radiography in all dogs at short-term follow-up period. Bony fusion was confirmed in 2/4 dogs at 12 months post-surgery and in 2/2 dogs at 24 months surgery. Subsidence of the spacer at 3 months post-surgery was observed in 7/8 affected intervertebral disc spaces in 5/6 dogs at 3 months post-surgery. Minor complications included screw loosening in 1 dog at 4 months post-surgery, breakage of the screws in 1 dog at 6 months post-surgery, and breakage of locking plates in 1 dog at 18 months post-surgery. ASD was confirmed by MRI in 2 dogs at 17 months and 24months post-surgery, respectively. Based on the results of the morphometric analyses, I found that the cylindrical intervertebral spacers successfully spread the IVD space and intervertebral foramina immediately post-surgery, but the distraction effect could not be maintained long-term. Nevertheless, there was no deterioration of clinical signs and no revision surgery was required. These results suggested that the removal of a part of the annulus fibrosus and the dorsal longitudinal ligament, which compressed the ventral side of the spinal cord, prevented the deterioration of clinical sign due to early implant failure or subsidence of the intervertebral spacer. The importance of inserting intervertebral spacers is to restore the collapsed IVD space and to change the local environment that promotes bony fusion between adjacent bones to achieve the stabilization of the cervical spine. This study provided additional data to previous reports about the degree of spinal cord decompression and intervertebral distraction by intervertebral spacers in combination with locking plates. Additionally, it is suggested that the distraction and fusion technique reported in this study is clinically effective and may be applicable as a surgical treatment for DA-CSM.

In Chapters 2 and 3, the accuracy and safety of the new surgical technique using the patient-specific drill guide template for the treatment of the instability of the thoracolumbar and lumbosacral spine in dogs were evaluated in canine cadaveric spines and clinical cases. Freehand insertion of pins/screws and fixation of these implants with PMMA have been performed as a standard technique for the stabilization of the thoracolumbar and lumbosacral instability in dogs. Although freehand pin/screw insertion can damage vital structures and potentially cause serious complications, no safe and accurate intraoperative technique has been established for the stabilization of the thoracolumbar and lumbosacral spine. The objective of these studies was to develop a patient-specific drill guide template system as a new intraoperative supporting device for the pin/screw placement and to evaluate the accuracy and safety of the drill guide template system for the stabilization of the thoracolumbar and lumbosacral vertebrae in dogs. In the thoracolumbar spine, all drill holes were made safely in cadaveric spines. In 89.6% of the screws used in clinical cases, there was no penetration into the vertebral canal and the screws were placed safely, leading to improvement in clinical signs in all cases. In the lumbosacral spine, all drill holes were completely located within the bone in both cadaveric spinal specimens and clinical cases. A total of 12 screws were placed safely in 3 clinical cases, and clinical signs of these cases were also improved. These safe and accurate surgical techniques that do not require expensive intraoperative equipment may replace fixation techniques by freehand implant insertion that has been associated with serious complications. Deviations of the drill holes from the planned trajectories may have been resulted from the change of the drill sleeve angle due to the load during drilling, which could be overcome by modifying the drill sleeve with more rigid materials. Another intrinsic disadvantage of the surgical techniques using the drill guide templates includes the requirement for the nearly complete removal of soft tissues from vertebrae to fit the template. Both of these drawbacks of the proposed surgical technique should be addressed in the future study in order to fully apply the technique to clinical cases.

In conclusion, I demonstrated that distraction and fusion surgery is a clinically effective surgical technique in canine cervical spinal instability. Morphometric analyses revealed that spinal cord compression and nerve root compression were reduced by spacer insertion to the affected IVD space. This research also provided data that the use of the patient-specific drill guide templates as an intraoperative support device is beneficial in that implant placement can be performed safely, accurately and at low cost in the surgical treatment of canine thoracolumbar and lumbosacral spinal instability.

Acknowledgments

I would like to express my deep gratitude to Professors Hiroaki Kamishina, Masaaki Katayama and Sadatoshi Maeda for their generous guidance and support in the preparation of my research.

I would like to express my deep gratitude to Dr. Taku Sugawara, the Director of Department of Spinal Surgery, Akita Cerebrospinal and Cardiovascular Center, Mr. Naoyuki Konno, Konno 3D Design, and Ms. Etsuko Ayaka, Ammtec Inc. for guidance in carrying out this research.

I would like to express my sincere gratitude to all the students and technical assistants of the Veterinary Clinical Radiology Laboratory, Gifu University, for their generous cooperation in my research.

References

1) Adams, M. A., McMillan, D. W., Green, T. P. and Dolan, P. (1996). Sustained loading generates stress concentrations in lumbar intervertebral discs. Spine (Phila Pa 1976). 21, 434-438.

2) Adams, M. A. and Roughley, P. J. (2006). What is intervertebral disc degeneration, and what causes it? Spine (Phila Pa 1976). 31, 2151-2161.

3) Adams, M. A., Hutton, W.C. (1988). *Mechanics of the intervertebral disc. In: The Biology of the Intervertebral Disc, First Ed., vol 2.* Boca Raton Florida: CRC Press, Inc.,.

4) Agnello, K. A., Kapatkin, A. S., Garcia, T. C., Hayashi, K., Welihozkiy, A. T. and Stover, S. M. (2010). Intervertebral biomechanics of locking compression plate monocortical fixation of the canine cervical spine. Vet Surg. 39, 991-1000.

5) Aikawa, T., Kanazono, S., Yoshigae, Y., Sharp, N. J. and Munana, K. R. (2007). Vertebral stabilization using positively threaded profile pins and polymethylmethacrylate, with or without laminectomy, for spinal canal stenosis and vertebral instability caused by congenital thoracic vertebral anomalies. Vet Surg. 36, 432-441.

6) Auger, J., Dupuis, J., Quesnel, A. and Beauregard, G. (2000). Surgical treatment of lumbosacral instability caused by discospondylitis in four dogs. Vet Surg. 29, 70-80.

7) Bakhsheshian, J., Mehta, V. A. and Liu, J. C. (2017). Current Diagnosis and Management of Cervical Spondylotic Myelopathy. Global Spine J. 7, 572-586.

8）Baskin, J. J., Vishteh, A. G., Dickman, C. A. and Sonntag, V. K. (1998). Techniques of anterior cervical plateing. Oper Tech Neurosurg. 1(2), 90-102.
9）Bergknut, N., Auriemma, E., Wijsman, S., Voorhout, G., Hagman, R., Lagerstedt, A. S., Hazewinkel, H. A. and Meij, B. P. (2011). Evaluation of intervertebral disk degeneration in chondrodystrophic and nonchondrodystrophic dogs by use of Pfirrmann grading of images obtained with low-field magnetic resonance imaging. Am J Vet Res. 72, 893-898.
10）Bergknut, N., Smolders, L. A., Grinwis, G. C., Hagman, R., Lagerstedt, A. S., Hazewinkel, H. A., Tryfonidou, M. A. and Meij, B. P. (2013). Intervertebral disc degeneration in the dog. Part 1: Anatomy and physiology of the intervertebral disc and characteristics of intervertebral disc degeneration. Vet J. 195, 282-291.
11）Bergman, R. L., Levine, J. M., Coates, J. R., Bahr, A., Hettlich, B. F. and Kerwin, S. C. (2008). Cervical spinal locking plate in combination with cortical ring allograft for a one level fusion in dogs with cervical spondylotic myelopathy. Vet Surg. 37, 530-536.
12）Blass, C. E. and Seim, H. B. (1984). Spinal fixation in dogs using Steinman pins and methymethacrylate. Vet Surg. 13, 203-210.
13）Blass, C. E., Waldron, D. R. and RT., V. E. (1988). Cervical stabilization in three dogs using steinmann pins and methyl methacrylate. J Am Anim Hosp Assoc. 24, 61-68.
14）Braund, K. G., Ghosh, P., Taylor, T. K. and Larsen, L. H. (1975). Morphological studies of the canine intervertebral disc. The assignment of the beagle to the achondroplastic classification. Res Vet Sci. 19, 167-172.

15）Brisson, B. A. (2010). Intervertebral disc disease in dogs. Vet Clin North Am Small Anim Pract. 40, 829-858.
16）Bruecker, K. A., Seim, H. B., 3rd and Withrow, S. J. (1989). Clinical evaluation of three surgical methods for treatment of caudal cervical spondylomyelopathy of dogs. Vet Surg. 18, 197-203.
17）Buckwalter, J. A. (1995). Aging and degeneration of the human intervertebral disc. Spine (Phila Pa 1976). 20, 1307-1314.
18）Bundoc, R. C., Delgado, G. G. and Grozman, S. A. (2017). A Novel Patient-Specific Drill Guide Template for Pedicle Screw Insertion into the Subaxial Cervical Spine Utilizing Stereolithographic Modelling: An In Vitro Study. Asian Spine J. 11, 4-14.
19）Cong, Y., Bao, N., Zhao, J. and Mao, G. (2015). Comparing Accuracy of Cervical Pedicle Screw Placement between a Guidance System and Manual Manipulation: A Cadaver Study. Med Sci Monit. 21, 2672-2677.
20）Cook, J. L., Evans, R., Conzemius, M. G., Lascelles, B. D., McIlwraith, C. W., Pozzi, A., Clegg, P., Innes, J., Schulz, K., Houlton, J., Fortier, L., Cross, A. R., Hayashi, K., Kapatkin, A., Brown, D. C. and Stewart, A. (2010). Proposed definitions and criteria for reporting time frame, outcome, and complications for clinical orthopedic studies in veterinary medicine. Vet Surg. 39, 905-908.
21）Corlazzoli, D. (2008). Bicortical implant insertion in caudal cervical spondylomyelopathy: a computed tomography simulation in affected Doberman Pinschers. Vet Surg. 37, 178-185.
22）da Costa, R. C., Parent, J. M., Partlow, G., Dobson, H., Holmberg, D. L. and Lamarre, J. (2006). Morphologic and morphometric magnetic resonance imaging

features of Doberman Pinschers with and without clinical signs of cervical spondylomyelopathy. Am J Vet Res. 67, 1601-1612.

23）da Costa, R. C. and Parent, J. M. (2007). One-year clinical and magnetic resonance imaging follow-up of Doberman Pinschers with cervical spondylomyelopathy treated medically or surgically. J Am Vet Med Assoc. 231, 243-250.

24）da Costa, R. C., Parent, J. M., Holmberg, D. L., Sinclair, D. and Monteith, G. (2008). Outcome of medical and surgical treatment in dogs with cervical spondylomyelopathy: 104 cases (1988-2004). J Am Vet Med Assoc. 233, 1284-1290.

25）Dai, L. (1998). Disc degeneration and cervical instability. Correlation of magnetic resonance imaging with radiography. Spine (Phila Pa 1976). 23, 1734-1738.

26）Dai, L. (1998). The relationship between vertebral body deformity and disc degeneration in lumbar spine of the senile. Eur Spine J. 7, 40-44.

27）Danielsson, F. and Sjostrom, L. (1999). Surgical treatment of degenerative lumbosacral stenosis in dogs. Vet Surg. 28, 91-98.

28）De Decker, S., Caemaert, J., Tshamala, M. C., Gielen, I. M., Van Bree, H. J., Bosmans, T., Wegge, B. and Van Ham, L. M. (2011). Surgical treatment of disk-associated wobbler syndrome by a distractable vertebral titanium cage in seven dogs. Vet Surg. 40, 544-554.

29）De Risio, L., Thomas, W. B. and Sharp, N. J. (2000). Degenerative lumbosacral stenosis. Vet Clin North Am Small Anim Pract. 30, 111-132, vi.

30）De Risio, L., Sharp, N. J., Olby, N. J., Munana, K. R. and Thomas, W. B. (2001). Predictors of outcome after dorsal decompressive laminectomy for degenerative lumbosacral stenosis in dogs: 69 cases (1987-1997). J Am Vet Med Assoc. 219, 624-628.
31）Dernell, W. S., Van Vechten, B. J., Straw, R. C., LaRue, S. M., Powers, B. E. and Withrow, S. J. (2000). Outcome following treatment of vertebral tumors in 20 dogs (1986-1995). J Am Anim Hosp Assoc. 36, 245-251.
32）Dixon, B. C., Tomlinson, J. L. and Kraus, K. H. (1996). Modified distraction-stabilization technique using an interbody polymethyl methacrylate plug in dogs with caudal cervical spondylomyelopathy. J Am Vet Med Assoc. 208, 61-68.
33）Early, P., Mente, P., Dillard, S. and Roe, S. (2013). In vitro biomechanical comparison of the flexion/extension mobility of the canine lumbosacral junction before and after dorsal laminectomy and partial discectomy. Vet J. 196, 533-535.
34）Early, P., Mente, P., Dillard, S. and Roe, S. (2015). In vitro biomechanical evaluation of internal fixation techniques on the canine lumbosacral junction. PeerJ. 3, e1094.
35）Ellison, G. W., Seim, H. B., 3rd and Clemmons, R. M. (1988). Distracted cervical spinal fusion for management of caudal cervical spondylomyelopathy in large-breed dogs. J Am Vet Med Assoc. 193, 447-453.
36）Fujiwara, A., Lim, T. H., An, H. S., Tanaka, N., Jeon, C. H., Andersson, G. B. and Haughton, V. M. (2000). The effect of disc degeneration and facet joint osteoarthritis on the segmental flexibility of the lumbar spine. Spine (Phila Pa 1976). 25, 3036-3044.

37）Godde, T. and Steffen, F. (2007). Surgical treatment of lumbosacral foraminal stenosis using a lateral approach in twenty dogs with degenerative lumbosacral stenosis. Vet Surg. 36, 705-713.
38）Goring, R. L., Beale, B. S. and Faulkner, R. F. (1991). The inverted cone decompression technique: a surgical treatment for cervical vertebral instability "Wobbler Syndrome" in Doberman pinschers. Part 1. J Am Anim Hosp Assoc. 27, 403-409.
39）Goring, R. L., Beale, B. S. and Faulkner, R. F. (1991). The invert cone decompression technique: a surgical treatment for cervical vertebral instability "Wobbler syndrome" in Doberman pinshers. Part 1. J Am Anim Hosp Assoc. 27, 403-409.
40）Grant, J. P., Oxland, T. R., Dvorak, M. F. and Fisher, C. G. (2002). The effects of bone density and disc degeneration on the structural property distributions in the lower lumbar vertebral endplates. J Orthop Res. 20, 1115-1120.
41）Hall, D. A., Snelling, S. R., Ackland, D. C., Wu, W. and Morton, J. M. (2015). Bending strength and stiffness of canine cadaver spines after fixation of a lumbar spinal fracture-luxation using a novel unilateral stabilization technique compared to traditional dorsal stabilization. Vet Surg. 44, 94-102.
42）Hamilton-Bennett, S. E., Oxley, B. and Behr, S. (2018). Accuracy of a patient-specific 3D printed drill guide for placement of cervical transpedicular screws. Vet Surg. 47, 236-242.
43）Hansen, H. J. (1952). A pathologic-anatomical study on disc degeneration in dog, with special reference to the so-called enchondrosis intervertebralis. Acta Orthop Scand Suppl. 11, 1-117.

44）Hettlich, B. F., Fosgate, G. T., Levine, J. M., Young, B. D., Kerwin, S. C., Walker, M., Griffin, J. and Maierl, J. (2010). Accuracy of conventional radiography and computed tomography in predicting implant position in relation to the vertebral canal in dogs. Vet Surg. 39, 680-687.
45）Hettlich, B. F., Allen, M. J., Pascetta, D., Fosgate, G. T. and Litsky, A. S. (2013). Biomechanical comparison between bicortical pin and monocortical screw/polymethylmethacrylate constructs in the cadaveric canine cervical vertebral column. Vet Surg. 42, 693-700.
46）Hida, K., Iwasaki, Y., Yano, S., Akino, M. and Seki, T. (2008). Long-term follow-up results in patients with cervical disk disease treated by cervical anterior fusion using titanium cage implants. Neurol Med Chir (Tokyo). 48, 440-446; discussion 446.
47）Hilibrand, A. S. and Robbins, M. (2004). Adjacent segment degeneration and adjacent segment disease: the consequences of spinal fusion? Spine J. 4, 190S-194S.
48）Hirano, Y., Mizuno, J., Nakagawa, H., Itoh, Y., Kubota, K., Watanabe, S., Matsuoka, H., Numazawa, S., Tomii, M. and Watanabe, K. (2011). Minimally invasive central corpectomy for ossified posterior longitudinal ligament in the cervical spine. J Clin Neurosci. 18, 131-135.
49）Horner, H. A., Roberts, S., Bielby, R. C., Menage, J., Evans, H. and Urban, J. P. (2002). Cells from different regions of the intervertebral disc: effect of culture system on matrix expression and cell phenotype. Spine (Phila Pa 1976). 27, 1018-1028.

50）Jeffery, N. D. and McKee, W. M. (2001). Surgery for disc-associated wobbler syndrome in the dog--an examination of the controversy. J Small Anim Pract. 42, 574-581.
51）Jeffery, N. D. (2010). Vertebral fracture and luxation in small animals. Vet Clin North Am Small Anim Pract. 40, 809-828.
52）Joffe, M. R., Parr, W. C. H., Tan, C., Walsh, W. R. and Brunel, L. (2019). Development of a Customized Interbody Fusion Device for Treatment of Canine Disc-Associated Cervical Spondylomyelopathy. Vet Comp Orthop Traumatol. 32, 79-86.
53）Kahmann, R. D., Buttermann, G. R., Lewis, J. L. and Bradford, D. S. (1990). Facet loads in the canine lumbar spine before and after disc alteration. Spine (Phila Pa 1976). 15, 971-978.
54）Kaiser, M. G., Haid, R. W., Jr., Subach, B. R., Barnes, B. and Rodts, G. E., Jr. (2002). Anterior cervical plating enhances arthrodesis after discectomy and fusion with cortical allograft. Neurosurgery. 50, 229-236; discussion 236-228.
55）Kaneyama, S., Sugawara, T., Sumi, M., Higashiyama, N., Takabatake, M. and Mizoi, K. (2014). A novel screw guiding method with a screw guide template system for posterior C-2 fixation: clinical article. J Neurosurg Spine. 21, 231-238.
56）Kaneyama, S., Sugawara, T. and Sumi, M. (2015). Safe and accurate midcervical pedicle screw insertion procedure with the patient-specific screw guide template system. Spine (Phila Pa 1976). 40, E341-348.
57）Keller, T. S., Hansson, T. H., Abram, A. C., Spengler, D. M. and Panjabi, M. M. (1989). Regional variations in the compressive properties of lumbar vertebral trabeculae. Effects of disc degeneration. Spine (Phila Pa 1976). 14, 1012-1019.

58）Koehler, C. L., Stover, S. M., LeCouteur, R. A., Schulz, K. S. and Hawkins, D. A. (2005). Effect of a ventral slot procedure and of smooth or positive-profile threaded pins with polymethylmethacrylate fixation on intervertebral biomechanics at treated and adjacent canine cervical vertebral motion units. Am J Vet Res. 66, 678-687.
59）Kumaresan, S., Yoganandan, N., Pintar, F. A., Maiman, D. J. and Goel, V. K. (2001). Contribution of disc degeneration to osteophyte formation in the cervical spine: a biomechanical investigation. J Orthop Res. 19, 977-984.
60）Lu, S., Zhang, Y. Z., Wang, Z., Shi, J. H., Chen, Y. B., Xu, X. M. and Xu, Y. Q. (2012). Accuracy and efficacy of thoracic pedicle screws in scoliosis with patient-specific drill template. Med Biol Eng Comput. 50, 751-758.
61）M, N. (1994). Degenerative lumbosacral stenosis in the dog: a review of 30 cases. J Small Anim Pract. 35, 185-190.
62）Matsunaga, S., Kabayama, S., Yamamoto, T., Yone, K., Sakou, T. and Nakanishi, K. (1999). Strain on intervertebral discs after anterior cervical decompression and fusion. Spine (Phila Pa 1976). 24, 670-675.
63）McKee, W. M., Lavelle, R. B., Richardson, J. L. and al., e. (1990). Vertebral distraction- fusion for cervical spondylopathy using a screw and double washer technique. J Small Anim Pract. 31, 22-27.
64）McKee, W. M., Lavelle, R. B., Richardson, J. L. and al., e. (1990). Vertebral distraction-fusion for cervical spondylopathy using a screw and double washer technique. J Small Anim Pract. 31, 22-27.

65) McKee, W. M., Butterworth, S. J. and Scott, H. W. (1999). Management of cervical spondylopathy-associated intervertebral, disc protrusions using metal washers in 78 dogs. J Small Anim Pract. 40, 465-472.
66) McKee, W. M. and Sharp, N. J. (2003). *Cervical spondylopathy, in Slatter D (ed): Textbook of Small Animal Surgery (ed 3).* Philadelphia, PA: Saunders.
67) McNally, D. S. and Adams, M. A. (1992). Internal intervertebral disc mechanics as revealed by stress profilometry. Spine (Phila Pa 1976). 17, 66-73.
68) Meij, B. P., Suwankong, N., Van der Veen, A. J. and Hazewinkel, H. A. (2007). Biomechanical flexion-extension forces in normal canine lumbosacral cadaver specimens before and after dorsal laminectomy-discectomy and pedicle screw-rod fixation. Vet Surg. 36, 742-751.
69) Meij, B. P. and Bergknut, N. (2010). Degenerative lumbosacral stenosis in dogs. Vet Clin North Am Small Anim Pract. 40, 983-1009.
70) Miyamoto, H. and Uno, K. (2009). Cervical pedicle screw insertion using a computed tomography cutout technique. J Neurosurg Spine. 11, 681-687.
71) Miyata, M., Neo, M., Ito, H., Yoshida, M., Fujibayashi, S. and Nakamura, T. (2008). Rheumatoid arthritis as a risk factor for a narrow C-2 pedicle: 3D analysis of the C-2 pedicle screw trajectory. J Neurosurg Spine. 9, 17-21.
72) Miyata, M., Neo, M., Ito, H., Yoshida, M., Miyaki, K., Fujibayashi, S., Nakayama, T. and Nakamura, T. (2008). Is rheumatoid arthritis a risk factor for a high-riding vertebral artery? Spine (Phila Pa 1976). 33, 2007-2011.
73) Mizuno, J., Nakagawa, H., Song, J. and Matsuo, N. (2005). Surgery for dural ossification in association with cervical ossification of the posterior longitudinal ligament via an anterior approach. Neurol India. 53, 354-357.

74）Morrison, E. J., Litsky, A. S., Allen, M. J., Fosgate, G. T. and Hettlich, B. F. (2016). Evaluation of Three Human Cervical Fusion Implants for Use in the Canine Cervical Vertebral Column. Vet Surg. 45, 901-908.

75）Nakagawa, H. and Mizuno, J. (2004). *Threaded interbody cage fixation for cervical spondylosis and ossification of the posterior longitudinal ligament.* . Philadelphia: Elsevier Churchill Livingstone.

76）Nel, J. J., Kat, C. J., Coetzee, G. L. and van Staden, P. J. (2017). Biomechanical comparison between pins and polymethylmethacrylate and the SOP locking plate system to stabilize canine lumbosacral fracture-luxation in flexion and extension. Vet Surg. 46, 789-796.

77）Oegema, T. R., Jr. (2002). The role of disc cell heterogeneity in determining disc biochemistry: a speculation. Biochem Soc Trans. 30, 839-844.

78）Oxley, B. and Behr, S. (2016). Stabilisation of a cranial cervical vertebral fracture using a 3D-printed patient-specific drill guide. J Small Anim Pract. 57, 277.

79）Palmer, R. H. and Chambers, J. N. (1991). Canine lumbosacral disease Part Ⅱ: Definition, diagnosis, treasment, and prognosis. Comp Cont Ed. 13, 213-221.

80）Panjabi, M. M., White, A. A., 3rd, Keller, D., Southwick, W. O. and Friedlaender, G. (1978). Stability of the cervical spine under tension. J Biomech. 11, 189-197.

81）Queen, J. P., Coughlan, A. R., May, C., Bennett, D. and Penderis, J. (1998). Management of disc-associated wobbler syndrome with a partial slot fenestration and position screw technique. J Small Anim Pract. 39, 131-136.

82）Ramos, R. M., da Costa, R. C., Oliveira, A. L., Kodigudla, M. K. and Goel, V. K. (2015). Morphological changes of the caudal cervical intervertebral foramina due to flexion-extension and compression-traction movements in the canine cervical vertebral column. BMC Vet Res. 11, 184.
83）Rapoff, A. J., O'Brien, T. J., Ghanayem, A. J., Heisey, D. M. and Zdeblick, T. A. (1999). Anterior cervical graft and plate load sharing. J Spinal Disord. 12, 45-49.
84）Reints Bok, T. E., Willemsen, K., van Rijen, M. H. P., Grinwis, G. C. M., Tryfonidou, M. A. and Meij, B. P. (2019). Instrumented cervical fusion in nine dogs with caudal cervical spondylomyelopathy. Vet Surg. 48, 1287-1298.
85）Rohner, D., Kowaleski, M. P., Schwarz, G. and Forterre, F. (2019). Short-Term Clinical and Radiographical Outcome after Application of Anchored Intervertebral Spacers in Dogs with Disc-Associated Cervical Spondylomyelopathy. Vet Comp Orthop Traumatol. 32, 158-164.
86）Roughley, P. J. (2004). Biology of intervertebral disc aging and degeneration: involvement of the extracellular matrix. Spine (Phila Pa 1976). 29, 2691-2699.
87）Rusbridge, C., Wheeler, S. J., Torrington, A. M., Pead, M. J. and Carmichael, S. (1998). Comparison of two surgical techniques for the management of cervical spondylomyelopathy in dobermanns. J Small Anim Pract. 39, 425-431.
88）Salger, F., Ziegler, L., Böttcher, I. C., Oechtering, G., Böttcher, P. and Flegel, T. (2014). Neurologic outcome after thoracolumbar partial lateral corpectomy for intervertebral disc disease in 72 dogs. Vet Surg. 43, 581-588.

89) Samartzis, D., Shen, F. H., Lyon, C., Phillips, M., Goldberg, E. J. and An, H. S. (2004). Does rigid instrumentation increase the fusion rate in one-level anterior cervical discectomy and fusion? Spine J. 4, 636-643.
90) Schollhorn, B., Burki, A., Stahl, C., Howard, J. and Forterre, F. (2013). Comparison of the biomechanical properties of a ventral cervical intervertebral anchored fusion device with locking plate fixation applied to cadaveric canine cervical spines. Vet Surg. 42, 825-831.
91) Seim, H. and Withrow, S. J. (1982). Pathophysiology and diagnosis of caudal cervical spondylo-myelopathy. J Am Anim Hosp Assoc. 18, 241-251.
92) Seim, H. B. and Withrow, S. J. (1982). Pathphysiology and diagnosis of caudal cervical spondylo-myelopathy with emphasis on the Doberman pinscher. J Am Anim Hosp Assoc. 18, 241-251.
93) Setton, L. A. and Chen, J. (2006). Mechanobiology of the intervertebral disc and relevance to disc degeneration. J Bone Joint Surg Am. 88 Suppl 2, 52-57.
94) Shamir, M. H., Chai, O. and Loeb, E. (2008). A method for intervertebral space distraction before stabilization combined with complete ventral slot for treatment of disc-associated wobbler syndrome in dogs. Vet Surg. 37, 186-192.
95) Shapiro, S. (1996). Banked fibula and the locking anterior cervical plate in anterior cervical fusions following cervical discectomy. J Neurosurg. 84, 161-165.
96) Shapiro, S., Connolly, P., Donnaldson, J. and Abel, T. (2001). Cadaveric fibula, locking plate, and allogeneic bone matrix for anterior cervical fusions after cervical discectomy for radiculopathy or myelopathy. J Neurosurg. 95, 43-50.
97) Smit, T. H. (2002). The use of a quadruped as an in vivo model for the study of the spine - biomechanical considerations. Eur Spine J. 11, 137-144.

98) Smolders, L. A., Bergknut, N., Kingma, I., van der Veen, A. J., Smit, T. H., Koole, L. H., Hazewinkel, H. A. and Meij, B. P. (2012). Biomechanical evaluation of a novel nucleus pulposus prosthesis in canine cadaveric spines. Vet J. 192, 199-205.

99) Smolders, L. A., Kingma, I., Bergknut, N., van der Veen, A. J., Dhert, W. J., Hazewinkel, H. A., van Dieen, J. H. and Meij, B. P. (2012). Biomechanical assessment of the effects of decompressive surgery in non-chondrodystrophic and chondrodystrophic canine multisegmented lumbar spines. Eur Spine J. 21, 1692-1699.

100) Smolders, L. A., Voorhout, G., van de Ven, R., Bergknut, N., Grinwis, G. C., Hazewinkel, H. A. and Meij, B. P. (2012). Pedicle screw-rod fixation of the canine lumbosacral junction. Vet Surg. 41, 720-732.

101) Solano, M. A., Fitzpatrick, N. and Bertran, J. (2015). Cervical Distraction-Stabilization Using an Intervertebral Spacer Screw and String-of Pearl (SOP) Plates in 16 Dogs With Disc-Associated Wobbler Syndrome. Vet Surg. 44, 627-641.

102) Steffen, F., Voss, K. and Morgan, J. P. (2011). Distraction-fusion for caudal cervical spondylomyelopathy using an intervertebral cage and locking plates in 14 dogs. Vet Surg. 40, 743-752.

103) Sturges, B. K., Kapatkin, A. S., Garcia, T. C., Anwer, C., Fukuda, S., Hitchens, P. L., Wisner, T., Hayashi, K. and Stover, S. M. (2016). Biomechanical Comparison of Locking Compression Plate versus Positive Profile Pins and Polymethylmethacrylate for Stabilization of the Canine Lumbar Vertebrae. Vet Surg. 45, 309-318.

104) Sugawara, T., Itoh, Y., Hirano, Y., Higashiyama, N. and Mizoi, K. (2009). Long term outcome and adjacent disc degeneration after anterior cervical discectomy and fusion with titanium cylindrical cages. Acta Neurochir (Wien). 151, 303-309; discussion 309.
105) Sugawara, T., Higashiyama, N., Kaneyama, S., Takabatake, M., Watanabe, N., Uchida, F., Sumi, M. and Mizoi, K. (2013). Multistep pedicle screw insertion procedure with patient-specific lamina fit-and-lock templates for the thoracic spine: clinical article. J Neurosurg Spine. 19, 185-190.
106) Suwankong, N., Meij, B. P., Van Klaveren, N. J., Van Wees, A. M., Meijer, E., Van den Brom, W. E. and Hazewinkel, H. A. (2007). Assessment of decompressive surgery in dogs with degenerative lumbosacral stenosis using force plate analysis and questionnaires. Vet Surg. 36, 423-431.
107) Swaim, S. F. (1975). Evaluation of four techniques of cervical spinal fixation in dogs. J Am Vet Med Assoc. 166, 1080-1086.
108) Tellegen, A. R., Willems, N., Tryfonidou, M. A. and Meij, B. P. (2015). Pedicle screw-rod fixation: a feasible treatment for dogs with severe degenerative lumbosacral stenosis. BMC Vet Res. 11, 299.
109) Teunissen, M., van der Veen, A. J., Smit, T. H., Tryfonidou, M. A. and Meij, B. P. (2017). Effect of a titanium cage as a stand-alone device on biomechanical stability in the lumbosacral spine of canine cadavers. Vet J. 220, 17-23.
110) Tian, N. F., Huang, Q. S., Zhou, P., Zhou, Y., Wu, R. K., Lou, Y. and Xu, H. Z. (2011). Pedicle screw insertion accuracy with different assisted methods: a systematic review and meta-analysis of comparative studies. Eur Spine J. 20, 846-859.

111）Trotter, E. J. (1986). *Canine wobbler syndrome*. Philadelphia, PA: Saunders.
112）Trotter, E. J. (2009). Cervical spine locking plate fixation for treatment of cervical spondylotic myelopathy in large breed dogs. Vet Surg. 38, 705-718.
113）VanGundy, T. E. (1988). Disc-associated wobbler syndrome in the Doberman pinscher. Vet Clin North Am Small Anim Pract. 18, 667-696.
114）Voss, K., Steffen, F. and Montavon, P. M. (2006). Use of the ComPact UniLock System for ventral stabilization procedures of the cervical spine: a retrospective study. Vet Comp Orthop Traumatol. 19, 21-28.
115）Walker, T. M., Pierce, W. A. and Welch, R. D. (2002). External fixation of the lumbar spine in a canine model. Vet Surg. 31, 181-188.
116）Watine, S., Cabassu, J. P., Catheland, S., Brochier, L. and Ivanoff, S. (2006). Computed tomography study of implantation corridors in canine vertebrae. J Small Anim Pract. 47, 651-657.
117）Watt, P. R. (1991). Degenerative lumbosacral stenosis in 18 dogs. J Small Anim Pract. 32, 125-134.
118）Weh, J. M. and Kraus, K. H. (2007). Use of a four pin and methylmethacrylate fixation in L7 and the iliac body to stabilize lumbosacral fracture-luxations: a clinical and anatomic study. Vet Surg. 36, 775-782.
119）Wheeler, J. L., Cross, A. R. and Rapoff, A. J. (2002). A comparison of the accuracy and safety of vertebral body pin placement using a fluoroscopically guided versus an open surgical approach: an in vitro study. Vet Surg. 31, 468-474.
120）Wheeler, J. L., Lewis, D. D., Cross, A. R. and Sereda, C. W. (2007). Closed fluoroscopic-assisted spinal arch external skeletal fixation for the stabilization of vertebral column injuries in five dogs. Vet Surg. 36, 442-448.

121）Wheeler, S. J. (1992). Lumbosacral disease. Vet Clin North Am Small Anim Pract. 22, 937-950.

122）Wheeler, S. J. and Sharp, N. J. (2005). *Small Animal Spinal Disorders* (Vol. 32). Philadelphia, PA: Elsevier-Mosby.

123）White, A. A. and Panjabi, M. (1978). *Clinical Biomechanics of the Spine.* Philadelphia, Toronto: Lippincott Company.

124）Yukawa, Y., Kato, F., Ito, K., Horie, Y., Hida, T., Nakashima, H. and Machino, M. (2009). Placement and complications of cervical pedicle screws in 144 cervical trauma patients using pedicle axis view techniques by fluoroscope. Eur Spine J. 18, 1293-1299.

125）Zaveri, G. R. and Ford, M. (2001). Cervical spondylosis: the role of anterior instrumentation after decompression and fusion. J Spinal Disord. 14, 10-16.

126）Zimmerman, M. C., Vuono-Hawkins, M., Parsons, J. R., Carter, F. M., Gutteling, E., Lee, C. K. and Langrana, N. A. (1992). The mechanical properties of the canine lumbar disc and motion segment. Spine (Phila Pa 1976). 17, 213-220.

127）Zindl, C., Litsky, A. S., Fitzpatrick, N. and Allen, M. J. (2018). Kinematic behavior of a novel pedicle screw-rod fixation system for the canine lumbosacral joint. Vet Surg. 47, 114-124.